Quaternary International xxx (2016) 1–19

Contents lists available at ScienceDirect

Quaternary International

journal homepage: www.elsevier.com/locate/quaint

Analysis of the interaction between neotectonic and surface processes in a low-land intracratonic setting of South America

Ernesto Brunetto [a, *], Daniela M. Kröhling [b, c], María Cecilia Zalazar [c], María Candela Francisconi [c]

[a] CICyTTP-CONICET, Dr. Materi y España sn, 3105 Diamante, Entre Ríos, Argentina
[b] CONICET, Argentina
[c] Universidad Nacional del Litoral, CC 217, 3000 Santa Fe, Argentina

ARTICLE INFO

Article history:
Available online xxx

Keywords:
Tectonic Geomorphology
Intracratonic settings
Late Pleistocene/Holocene
Fluvial incision rates
Low uplift rate regions

ABSTRACT

The Quaternary sedimentary record in the continental interiors has generally been studied taking into consideration the climatic forcing. However, episodes of uplift controlling the development of landforms have often been dismissed. The interiors of continents are typically considered to have low deformation rates, lower than the rates of exogenous processes. Deformation in the middle of the Pampean plains, an intracratonic setting of South America, has been observed to have generated an elevated area surrounded by lowland plains. This elevated area is susceptible to fluvial erosion. From this fact we developed a geomorphologic modelling constrained from geomorphic markers in order to estimate the relative incidence of the different factors that control erosion in lowland landscapes. An adapted erosion code was employed, which combines fluvial incision equation (the stream power law), an uplift function spatially distributed and the hillslope diffusion equation. A low-DEM was achieved for restoring an initial non-deformed topography affected by low fluvial incision. It represents a palaeosurface chrono-stratigraphically constrained. The estimation of the model parameters was achieved by applying the inversion method. The best-fit between the numerical solution (calculated topography) and the measured topography (simulated by means a DEM) was approached by comparison of the stream longitudinal profiles. The yield numerical approach suggests that a geomorphological modelling based on the stream power law is possible to be applied in low-land landscapes. For this, a large scale change of the magnitude of the processes modelling the landscape should be expected in comparison with mountain erosional environments. Remarkably low K empirical values ($K = 5 \times 10^{-6}$–6×10^{-6} yr^{-1}) suggest that the extremely low slopes exert a larger influence on the stream power in low-land landscapes. Also the diffusion coefficient D values resulted largely lower (3×10^{-4}–1.9×10^{-3} cm^2/yr) than presented in tectonically active landscapes (>0.03 cm^2/yr). Regional uplift rates can be higher (0.35 mm/yr) than it is generally expected in low uplift rate settings (0.1–0.25 mm/yr). These estimations evidence highly dynamic surface and tectonic processes controlling the landscape evolution over intermediate time scales in an intracratonic setting.

1. Introduction

An intracratonic basin is a broad area with low-relief and slow subsidence rates developed in continental crust away from plate margins (Klein, 1995). They are considered as acyclic areas where landforms and the sedimentary record are constantly reworked (Klein, 1995; Peulvast et al., 2009). Such continental interiors are typically considered to be tectonically inactive. However, extensive regions of stable continental lithosphere have experienced prolonged subsidence, interrupted by phases of uplift (Armitage and Allen, 2010). The long-term subsidence history cannot be considered as a linear process because the cratonic basin-fill is responding to changes in the far field plate boundary regions (such as flexure and in-plane stress) and mantle dynamics (Armitage and Allen, 2010). For example, episodes of uplift have occurred in the interior of a sedimentary environment because of

* Corresponding author.
E-mail address: ernestobrunetto@cicyttp.org.ar (E. Brunetto).

http://dx.doi.org/10.1016/j.quaint.2016.06.018
1040-6182/

flexural loading in foreland basins (De Celles and Giles, 1996; Horton and De Celles, 1997; Dávila et al., 2010) or by tectonic inversion occurring in midcontinent settings (Smalley et al., 2005). As a consequence, the resulting uplands located in sedimentary domains can constitute headwater areas susceptible to fluvial incision.

In addition, the Quaternary sedimentary record in intracratonic settings has been mainly studied over intermediate timescales of landscape evolution (1×10^5–1×10^6 yr) in the context of exogenous processes. Controls such as climatic forcing that rule out rock erosion, velocity of streams or winds and sedimentary flux and sea-level change have been largely analysed (Walling and Webb, 1996; Blum and Törnqvist, 2000; Paola, 2000). However, in intracratonic basins, where sedimentary accumulation has dominated for a long-time (1×10^7–1×10^8 yr), Quaternary uplift episodes have generally been dismissed.

Studies that report evidence of Quaternary tectonic deformation in intraplate settings are progressively growing (Talwani, 2014 and references therein). In South America, most of the Quaternary deformation has been reported in the Brazilian Shield, mainly in Precambrian basement rocks related to reactivations of geologically old structures (Riccomini et al., 1989; Assumpção, 1992; Saadi, 1993; Riccomini and Assumpção, 1999; Bezerra and Vita-Finzi, 2000; Saadi et al., 2002, 2005; Bezerra et al., 2006, 2008). A few examples referring to a clearly sedimentary domain were reported from the Amazonas River basin (Assumpção and Suarez, 1988; Cunha, 1988).

In the last years, with the development of the geomorphometry applied to geomorphology and morphotectonics, a number of exhaustive data were gathered from Digital Elevation Models (DEM), especially in intracratonic regions. Grohmann (2004, 2005) developed morphometric maps and a trend-surface analysis on data from morphometric parameters (hypsometry, slope, aspect, swath profiles, lineaments and drainage density, surface roughness, isobase and hydraulic gradient) in the south São Francisco Craton, Southeastern Brazil. Grohmann et al. (2007) generated also in this region a morphotectonic analysis of the Poços de Caldas Massif, a Late Cretaceous collapsed volcanic caldera. Recently Kröhling et al. (2014) deduced that morphometric analysis is an appropriate method for the reconstruction of long-term landscape development of the Paraná Basaltic Plateau (Northeastern Argentina and Southern Brazil). The authors included a first correlation of the main recognised discrete erosion palaeosurfaces to the main uplift episodes post-break-up of Gondwana. Complementary, independent approaches for identifying recent deformations are now available by applying geodetic tools such as measurements of tiny displacements from permanent GPS stations (Alves et al., 2003; Marotta et al., 2013; Sobrero and Brunetto, 2015). This information dealing with Tectonic Geomorphology issues holds a great potential but it needs to be integrally analysed.

More broadly, most of the works studying tectonics and fluvial incision have been developed for tectonically active mountain environments (Seidl and Dietrich, 1992; Whipple and Tucker, 1999; Whipple, 2004; Whipple and Meade, 2004; Gasparini and Brandon, 2011). For this propose, the classical stream power equation (SPL) is commonly used for describing the rate of fluvial incision (Howard and Kerby, 1983; Whipple and Tucker, 1999). The SPL assumes that parameters are kept constant over time and space, e.g. lithology and precipitation (Whipple and Tucker, 1999). It is also assumed that incision occurs in bedrock rivers which are usually steeper and lacking a sediment cover. This is the case of detachment-limited river channels, where it is the resistance to erosion that limits the rate of incision (Braun and Willett, 2013). Alluvial rivers have a lower gradient and have an inverse dependence upon drainage area (Howard and Kerby, 1983). They correspond to a transport-limited state, where it is the ability of the river to transport sediment that limits its evolution (Braun and Willett, 2013). This widely accepted generalisation does not consider the case of headwater systems located within low relief sedimentary plain settings (Iriondo and Drago, 2004), where a complex succession of endogenous geomorphic processes could have been operating, even during the geological evolution over an intermediate-time scale. As the channel transport ability exceeds supply, we can consider that channel incision in this case is limited primarily by the resistance of the underlying substratum to the boundary shear stress imposed by stream flows (Seidl and Dietrich, 1992).

Most of the previous research on low uplift rate in intracratonic settings is lacking comprehensive modelling approaches. They are mainly concern about detection of neotectonic activity through geomorphic indices. Recent quantitative approaches have been achieved in lowland areas of Northwestern Europe that shows the effects of tectonics on the landforms and streams in intraplate areas with low uplift rates (Lagarde et al., 2000, 2003; Lague et al., 2000; Font et al., 2010). The sensitivity of river profiles to detect changes in areas of low uplift rate has also been analysed from gradient variations of river profiles crossing different uplift zones in the Southern Upper Rhine Graben (Carretier et al., 2006).

New studies about the geological evolution of the Northern Pampa in Argentina during the Late Pleistocene have arisen from a geologically integrated approach (Brunetto, 2008; 2012; Brunetto et al., 2010; 2015a). Previously, evidence of Quaternary tectonic activity had been reported in this region from the observation of Late Pleistocene palaeostreams that were perturbed by reactivation of inferred faults (Pasotti, 1974, 1975). But those descriptive studies are lacking a quantitative understanding. A preliminary analysis of one longitudinal profile was tested in the Northern Pampa region in order to identify areas of potential differential uplift (Brunetto, 2008). Anomalies on the stream channel were detected by estimating the stream length index (SL) and the local slope index (S) considering the drainage area for each reach of the stream. However, this partial analysis was not able to discriminate an unequivocal tectonic origin for the anomalies, rather than a lithologic control.

Studies that define rates of erosion and uplift are the main concern of the Tectonic Geomorphology. They typically include geochronology, structure, stratigraphy, geomorphology, and numerical modelling (Burbank and Anderson, 2001). If recent deformation is recognized for low uplift rate settings, a calibration of the rates and relative contributions of each process at a particular time or over some span of time is pending to be achieved. The modern interdisciplinary research in intracratonic settings needs to start this way over shorter timescales.

The Northern Pampa plain case study can be useful to generate a discussion about how the different factors that control erosion/sedimentation in the landscape evolution interplays with tectonic activity in lowland regions, on an intermediate-time scale (1×10^5 yr). The preliminary research presented so far suggests that deformation rates seem to be much higher than previously envisaged in such geological settings.

In this contribution, we try to make a comparison between geomorphic and tectonic rates in order to understand the relative magnitude of the factors that interact for modelling the surface. Geomorphologic modelling is presented, by applying an erosion code that includes uplift, flexural scarp generation, diffusion of sediments and fluvial incision in a representative catchment basin located in the Chaco-Paraná intracratonic basin. The aim of the paper is to obtain a preliminary numerical model of the landscape evolution in a region of widespread low relief plains affected by Quaternary tectonics.

Please cite this article in press as: Brunetto, E., et al., Analysis of the interaction between neotectonic and surface processes in a low-land intracratonic setting of South America, Quaternary International (2016), http://dx.doi.org/10.1016/j.quaint.2016.06.018

To achieve this, an empirical selection of parameters was approached by using the inverse method. We constrained the parameters of the SPL from geomorphic markers and stratigraphic and structural data. Finally, based on the obtained results, we have developed a discussion about why rapid geomorphic evolution can occurs over the intermediate time-scale in an intracratonic setting characterized by a long-term history of subsidence.

2. Geological setting

The Northern Pampa region is located in the Western Rio del Plata craton (Fig. 1). This area is composed of Precambrian rocks that constitute the crystalline basement of the Chaco-Paraná intracratonic basin (Rapela et al., 2007). This basin comprises a 5000 m thick sedimentary sequence. During the Mesozoic, extension and rifting linked to the break-up of the Gondwana supercontinent developed local depocenters (Uliana et al., 1989; Peate et al., 1990). A continental volcanic episode generated basaltic rocks that currently outcrop in a broad plateau extending into Southern Brazil, Eastern Paraguay, Northeastern Argentina and Western Uruguay. In the Northern Pampas region these basaltic lavas can be found at ca. 800 m depth in boreholes, thus forming part of the Chaco-Paraná basin fill. The lava beds appear as discontinuous horizontal basaltic layers or as diabase dykes and sills (Peate, 1997). During the Late Cretaceous-Early Paleogene the sedimentation was linked to the post rift thermal subsidence stage (Yrigoyen, 1999). Compression in the western margin of the South American Plate during late Cenozoic times intensified the construction of the Andes orogen and the Sierras Pampeanas range system (Fig. 1). In this plate segment, the orogenic process was conditioned by the flat-slab geometry of the subducted Nazca Plate (Jordan and Allmendinger, 1986; Ramos et al., 2002). The propagation of deformation far away from the ocean trench generated a broad distal foreland basin. The sedimentation in this region is controlled by subsidence mechanisms associated to flexural loads and dynamic topography linked to the flat-slab subduction process (Dávila et al., 2010; Dávila and Lithgow-Bertelloni, 2013).

Added to the mechanisms that configured the medium and long-wavelength topography, the Northern Pampa landscape has been locally shaped by Quaternary tectonic deformation. This process was responsible for building the main regional morphostructures: the tectonic depression of Mar Chiquita, the San Guillermo elevated block (SGEB) and the San Cristobal block (SCB) (Fig. 2) (Kröhling and Iriondo, 1999, 2003; Brunetto, 2008; Kröhling and Brunetto, 2013; Brunetto et al., 2014).

The main regional block (SGEB) was configured partially by uplift in the forebulge area of the foreland basin system because of flexural deformation generated by the tectonic loading of the Sierra de Córdoba range (Eastern Pampean ranges) (Brunetto, 2008; Dávila et al., 2010). Other components of regional uplift were produced by the accumulation of displacements on localized fault planes in the margins of the SGEB (Brunetto, 2008; Brunetto et al.,

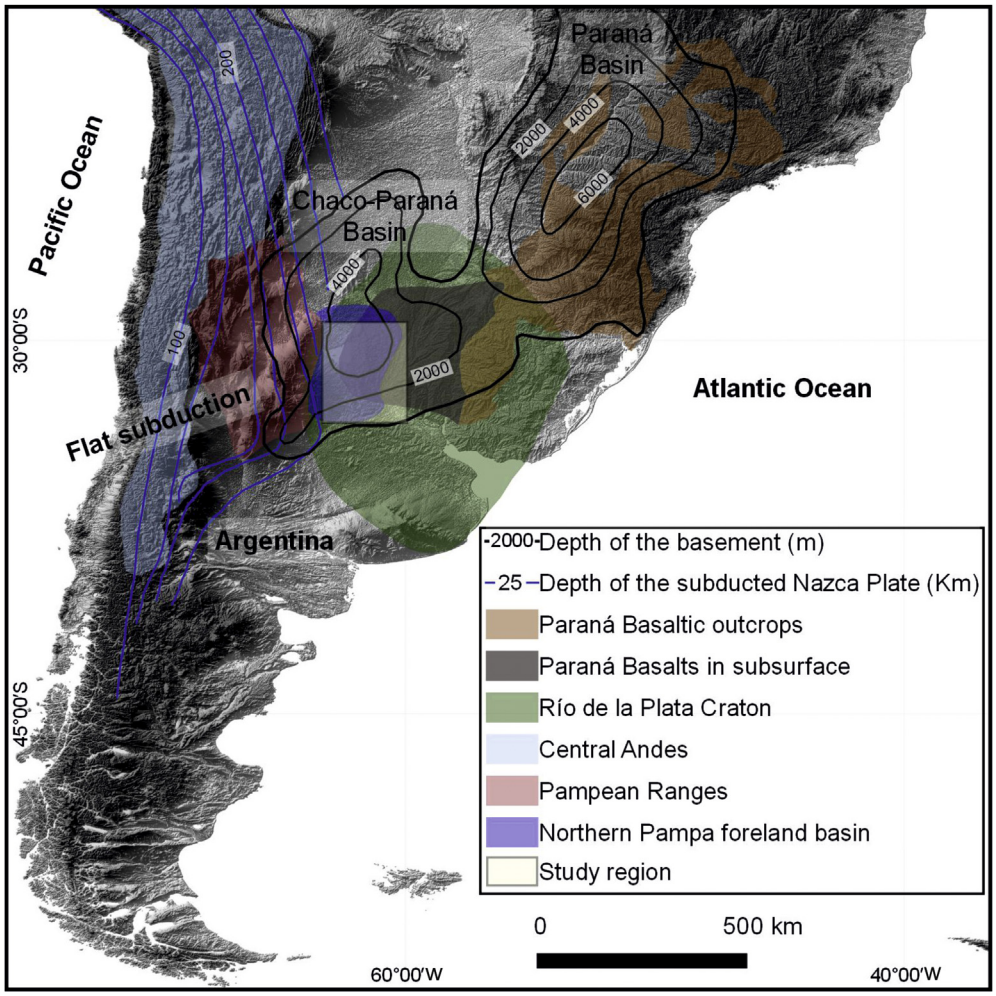

Fig. 1. Geological map of Southern South America (compiled from Milani and Zalán, 1999; Ramos, 1999; Rapela et al., 2007; Lagorio, 2008; Dávila et al., 2010).

Please cite this article in press as: Brunetto, E., et al., Analysis of the interaction between neotectonic and surface processes in a low-land intracratonic setting of South America, Quaternary International (2016), http://dx.doi.org/10.1016/j.quaint.2016.06.018

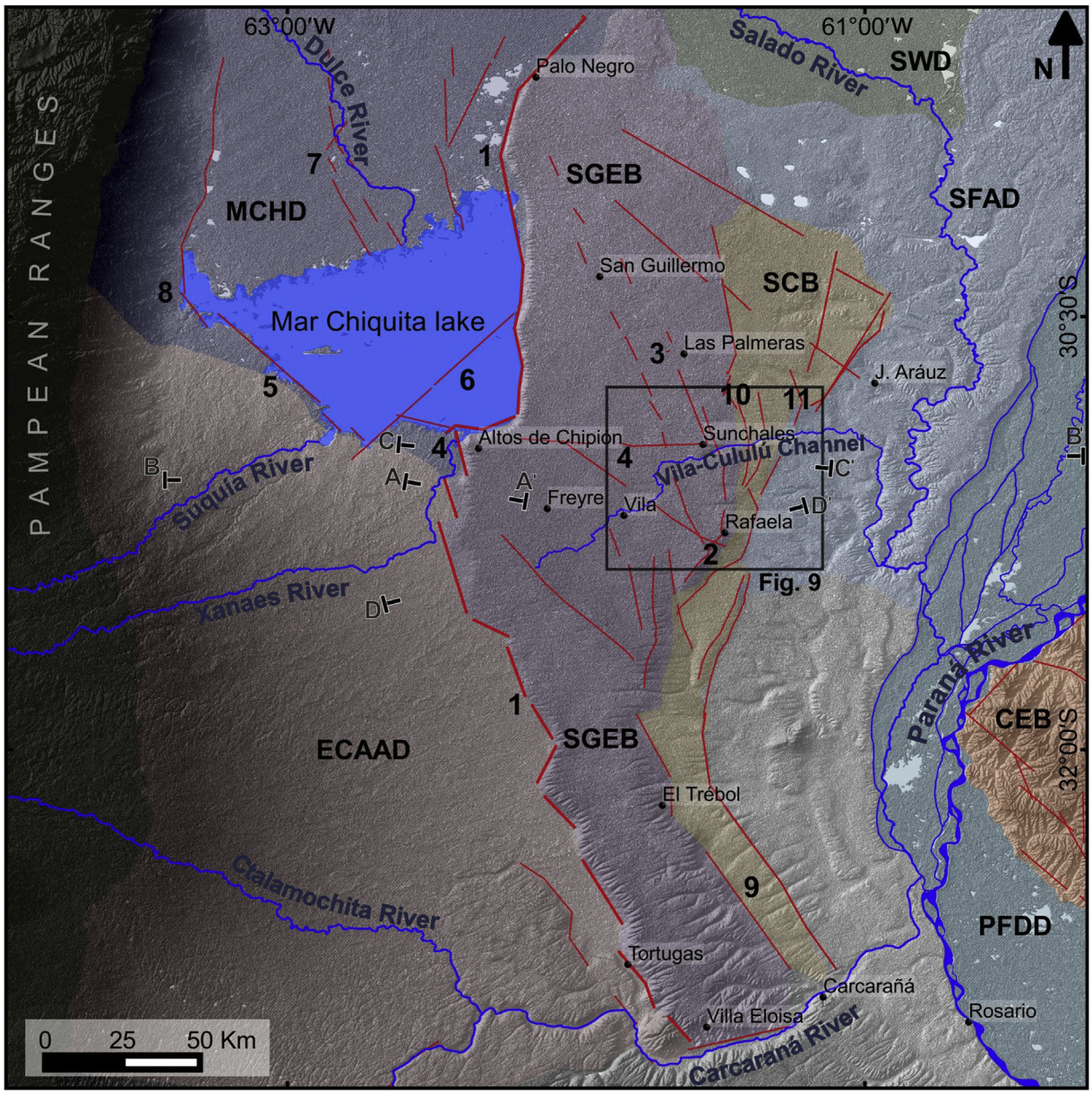

Fig. 2. Morphostructural Units defined in Northern Pampa region. SGEB: San Guillermo Elevated Block. SCB: San Cristobal Block. MCHD: Mar Chiquita Depression. ECAAD: Eastern Cordoba Alluvial Accumulation Depression. SFAD: Salado Fluvial Accumulation Depression. SWD: Salado Wetland Depression. PFDD: Paraná Fluvio-Deltaic Depression. CEB: Crespo Elevated Block. 1: Tostado-Selva Fault System (TSFS). 2: Rafaela Fault System (RFS). 3: Las Palmeras Fault. 4: Brinkmann-Sunchales Lineament. 5: Lagunilla del Plata Fault. 6: Balnearia Lineament. 7: Río Dulce Lineament. 8: Mar Chiquita Lineament. 9: El Trébol Fault. 10: Sunchales Fault System (SFS). 11: San Cristobal Fault System (SCFS). The black quadrate corresponds to the modelled area of Fig. 9.

2010). As Late Quaternary surface ruptures have not been observed, deformation was only inferred from indirect evidence including sharp deflections of stream channels, rectilinear features such as channel segments, hill ridges and shallow lake margins, and also, steeper slopes and gentle flexures on the ground. Relationships with older faults were discovered by interpreting seismic sections (Brunetto, 2008). It has been proposed that Quaternary faulting is linked to reverse mechanisms on blind faults that generate very gentle folds by fault-propagation (Fig. 3A). Deformation was suggested to be possible only by reactivation of pre-existing faults in this geodynamical context, which is characterised by low-strain rates (Brunetto et al., 2010; Brunetto and Giménez, 2012). There is no evidence of surface co-seismic displacements in the intracratonic region, except for the 1934 M 6.0 earthquake at the Sampacho town, a village situated in a lowland region closer the Eastern Pampean ranges. This site presents direct paleoseismological evidence that allow the inference of M $\geq$ 6.0 earthquakes (Costa et al., 2001; Sagripanti et al., 2011). Only three historically recorded earthquakes were reported along the Chaco-Pampean plain and the Río de la Plata craton (Brunetto, 2008; INPRES, 2010). But such a record lacks seismological and geological analyses. There is no local network of stations monitoring low-magnitude seismicity in the region.

The SGEB constitutes an extensive elevated plain 400 km long with a N–S orientation (Fig. 2). Tostado-Selva Fault System (TSFS), the main structure of the region, limits the SGEB on its western side (Pasotti and Castellanos, 1963; Pasotti, 1974; Iriondo, 1987; Kröhling and Iriondo, 2003; Brunetto, 2008; Brunetto et al.,

Please cite this article in press as: Brunetto, E., et al., Analysis of the interaction between neotectonic and surface processes in a low-land intracratonic setting of South America, Quaternary International (2016), http://dx.doi.org/10.1016/j.quaint.2016.06.018

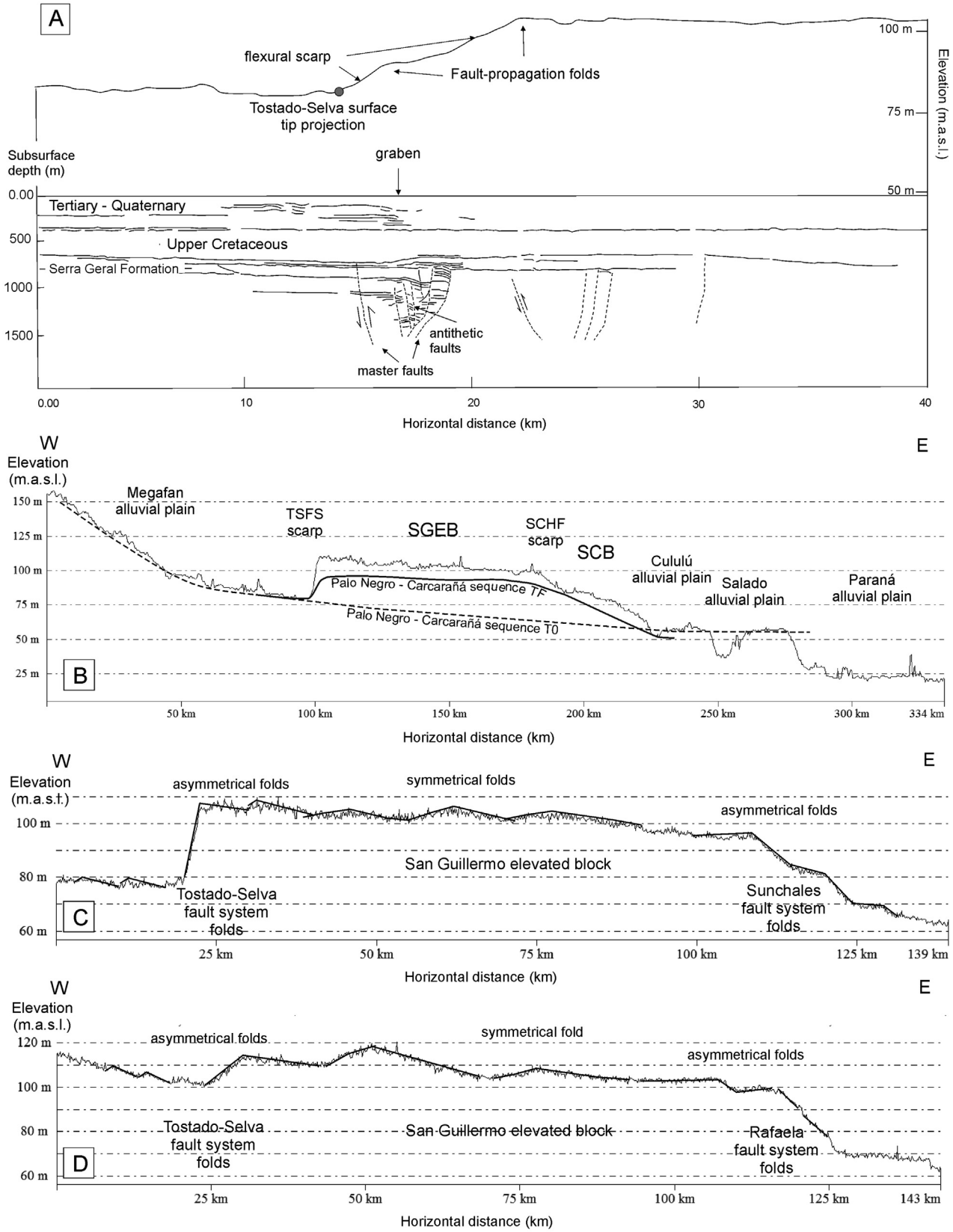

Fig. 3. A) Structural interpretation of the W–E cross section through TSFS (see location A–A′ profile in Fig. 2) (taken from Brunetto, 2008). B) W–E regional cross section through the main morphostructures (see location B–B′ profile in Fig. 2). In this, the Palo Negro – Carcarañá sequence is shown as a strain marker in the pre-deformation (To) and present (Tf) positions. C) W–E cross section through TSFS, SFS and SCFS (see location C–C′ profile in Fig. 2). D) W–E cross section through TSFS and RFS (see location D–D′ profile in Fig. 2).

Please cite this article in press as: Brunetto, E., et al., Analysis of the interaction between neotectonic and surface processes in a low-land intracratonic setting of South America, Quaternary International (2016), http://dx.doi.org/10.1016/j.quaint.2016.06.018

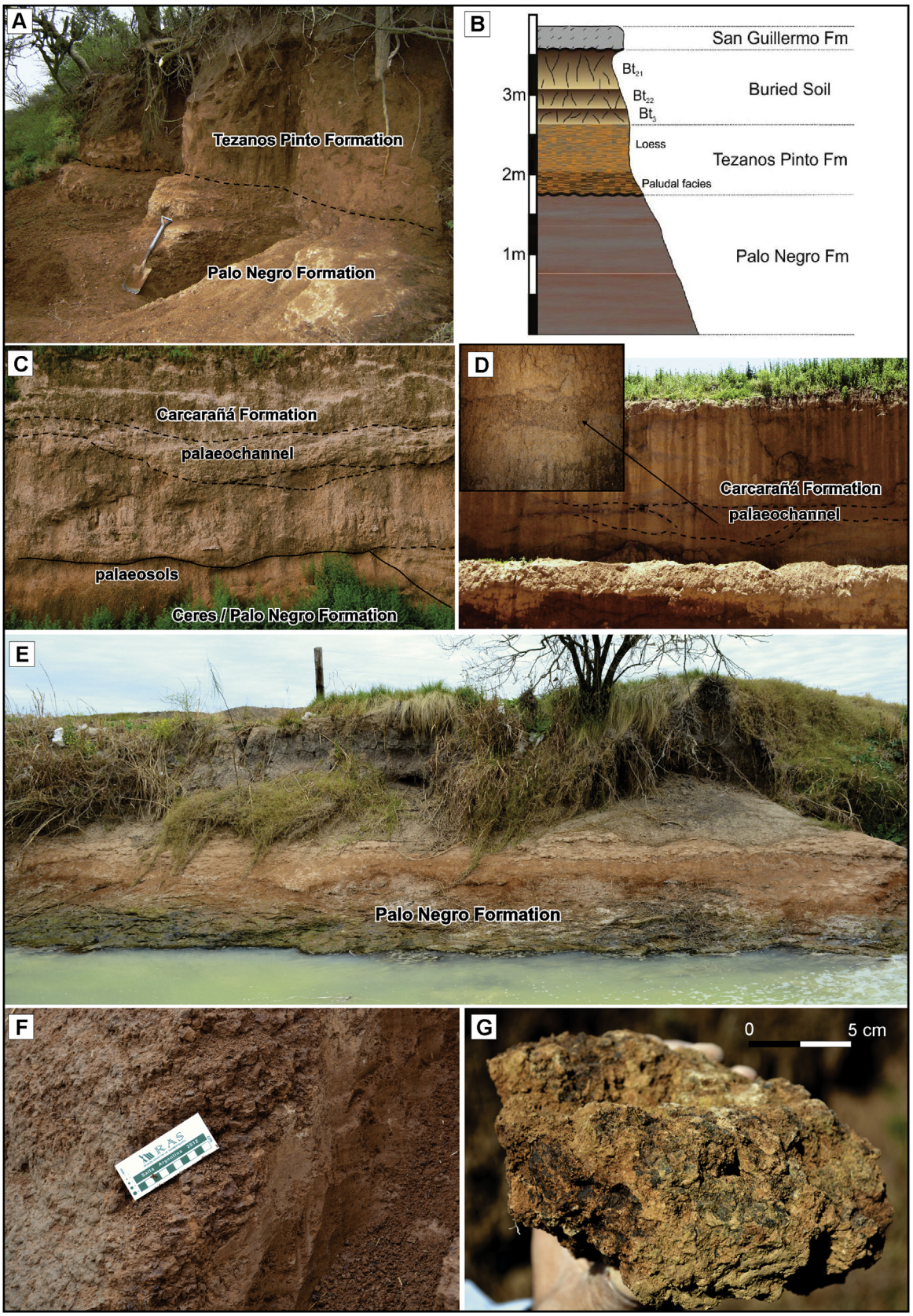

Fig. 4. A) Palo Negro Formation type profile (SGEB) (29°39′37″S; 62°08′54″W). B) Outcropping stratigraphic column representative of the study region (SGEB). C–D) Low energy fluvial facies of the Carcarañá Formation overlying the Ceres/Palo Negro Formation at the Tortugas site (southwestern SGEB) (32°43′35″S, 61°48′33″W). E) Outcropping sequence of the Vila-Cululú channel at the Eastern SGEB flexural scarp (30°57′17″S; 63°30′29″W). F–G) Typical facies of the Palo Negro Formation at Sunchales area (SGEB) (30°59′59″S, 61°37′7″W).

Please cite this article in press as: Brunetto, E., et al., Analysis of the interaction between neotectonic and surface processes in a low-land intracratonic setting of South America, Quaternary International (2016), http://dx.doi.org/10.1016/j.quaint.2016.06.018

2010). This fault system generated a gentle fold by fault-propagation (Brunetto et al., 2010) up to 40 m high, uplifting the western area of the SGEB (Fig. 3A). The Rafaela and El Trébol faults and correlative lineaments constitute the eastern limit of the SGEB (Kröhling and Iriondo, 2003) (Fig. 2). These structures generated multiple flexural scarps that reached up to 40 m of total vertical displacement. The SGEB is an overlying cover gently folded by faults with blind tip points.

3. Planar geomorphic markers

Identifiable geomorphic features or surfaces affected by tectonics can provide a reference frame for the analysis of the deformation. Geomorphic markers considered in this work are landforms, curviplanar surfaces and linear trends, in general marked by fluvial or lacustrine features, with known initial non-deformed geometries and relatively well estimated ages.

A Late Quaternary lithostratigraphic unit was formally defined in the region as Palo Negro Formation (Brunetto, 2008; Brunetto et al., 2010), and previously informally named as Ceres Formation (Kröhling, 1998; Kemp et al., 2004). This also was recognized from hidrogeological studies (Mannavella and Venencio, 1995). The Palo Negro Formation, interpreted as shallow lacustrine and ephemeral pond deposits by Brunetto et al. (2010), is a feature almost horizontal at the time of its formation. This flat lying sequence comprises a key regional stratigraphic marker because it outcrops along the flexural scarps generated by the TSFS (see locations in Fig. 2: Palo Negro, Altos de Chipión and Tortugas). At present, the top of this unit outcrops in natural profiles located at each side of the SGEB is at 76 m.a.s.l. (Western border) and 88 m.a.s.l. (Eastern border). As the structural slope of this palaeosurface was oriented eastward, such geodetic data suggest an uplift or/and tilting of the topography in the eastern side (Fig. 3B).

The type section of the unit was described in the Palo Negro quarry, in the northern extremity of the SGEB (Brunetto et al., 2010; Figs. 2 and 4A). It is composed of coarsely laminated clayey silts, that are dark brown (humid) to pale brown (dry) and structured into very coarse platy aggregates. The sedimentary bodies show discontinuous, sub-horizontal wavy lamination highlighted by the presence of horizontal carbonate plates. The post-depositional features were generated by chemical segregations mainly along primary lamination. Segregations also formed fine $CaCO_3$ rhizoconcretions and nodules. Abundant fine Fe-mottles are broadly scattered in the sediment; Fe/Mn-sesquioxides and clay films, and embedded sub-rounded dark brown silty aggregates are also present (Fig. 4). This facies displays a tabular architecture. At the Palo Negro site sediments were dated to 67 ka. B.P. (Brunetto et al., 2010; Table 1). The younger beds lie unconformably over the Palo Negro Formation, which suggests a period of erosion or no sedimentation (Fig. 4A,B).

Table 1
Summary of ages obtained on the outcropping Late Quaternary lithostratigraphic units representative of the studied region. *Ceres Formation correlated to Palo Negro Formation. **Sedimentary units assigned in this work to Tezanos Pinto Formation.

Formation	Site	Lab code	Burial depth (m)	TL age (ka)	OSL age (ka)	ISRL age (ka)	Reference
Palo Negro Fm	Palo Negro	UIC2109BL	2.2		67.4 ± 5.10		Brunetto et al. (2010)
Ceres Fm/Palo Negro Fm*	Tortugas	GL02006	6.4		145.6 ± 9.4		Kemp et al. (2004)
Ceres Fm/Palo Negro Fm*	Tortugas	ST139	7.3	91.9 ± 4.3			Kröhling (1998)
Ceres Fm/Palo Negro Fm*	Tortugas	GL02007	7.7		177.4 ± 12.0		Kemp et al. (2004)
Ceres Fm/Palo Negro Fm*	Tortugas	ST142	7.8	90.8 ± 9.1			Kröhling (1998)
Palo Negro Fm?	San Guillermo borehole	UIC2107BL	24.0		118.4 ± 7.6		Iriondo (2010)
Carcarañá Fm	Carcarañá	ST111	6.0	52.3 ± 0.1			Kröhling (1998, 1999)
Carcarañá Fm	Tortugas	GL02003	3.2		57.6 ± 2.9		Kemp et al. (2004)
Carcarañá Fm	Tortugas	GL02004	4.2		63.2 ± 3.4		Kemp et al. (2004)
Carcarañá Fm	Tortugas	GL02005	5.1		68.7 ± 3.7		Kemp et al. (2004)
Tezanos Pinto Fm**	Jacinto Aráuz	ST66	1.0	9.4 ± 0.6			Ramonell (*com. pers.*)
Tezanos Pinto Fm**	Rafaela	UniCologne	1.3			28.8 ± 2.9	Kruck et al. (2011)
Tezanos Pinto Fm	Tortugas	ST140	1.5	8.2 ± 0.4			Kröhling (1998)
Tezanos Pinto Fm	Tortugas	GL02002	1.8		23.3 ± 1.4		Kemp et al. (2004)
Tezanos Pinto Fm**	Freyre	LIAG	1.9			17.4 ± 1.5	Kruck et al. (2011)
Tezanos Pinto Fm**	Freyre	LIAG	2.2			18.6 ± 1.6	Kruck et al. (2011)
Tezanos Pinto Fm**	Rafaela	UniCologne	2.5			18.8 ± 3.2	Kruck et al. (2011)
Tezanos Pinto Fm	Altos de Chipión	–	3.0	32.0 ± 1.1			Kröhling and Iriondo (1999)
Tezanos Pinto Fm**	Freyre	LIAG	3.5			32.1 ± 2.7	Kruck et al. (2011)
Tezanos Pinto Fm	Carcarañá	ST95	3.8	31.7 ± 1.6			Kröhling (1999)
Tezanos Pinto Fm	Villa Eloísa	ST73	4.1	35.9 ± 1.0			Kröhling (1999)
Tezanos Pinto Fm	Rosario	–	4.8	32.0 ± 1.0			Kröhling (1998)
San Guillermo Fm	Tortugas	GL02001	0.2		1.0 ± 0.1		Kemp et al. (2004)

In the Tortugas quarry section, located at the southwestern extremity of the SGEB (Fig. 2), ephemeral lacustrine deposits, with precipitation of secondary carbonate and a capping hydromorphic paleosol, were assigned to the Ceres Formation (Fig. 4C). This unit was TL dated to ca. 92 ka. B.P (Kröhling, 1998). and OSL dated to 178–145 ka B.P. at the Tortugas site (Kemp et al., 2004; Table 1). The Ceres Formation correlates with the Palo Negro Formation.

Complementary stratigraphic evidence in the SGEB for the Quaternary-active character of the tectonic structures is represented by deposits of temporary swamps and small creeks (low energy river) and hydromorphic soils, outcropping in profiles along steepest slopes or under inactive palaeosurfaces (Fig. 4C–D).

The Carcarañá Formation was described in the southern area of the SGEB and dated to 52 ka. B.P. (MIS3) by Kröhling (1999). The formation is mainly composed of very fine to fine silty sand, with a reddish brown colour. Analysis of the sedimentary structures suggests that this unit is aeolian in origin, and was generated by dune dissipation processes, as a result of reworking by erosion of the dune fields that had developed in the Pampas region probably during MIS4 (Kröhling, 1998, 1999). A paleosol on top of the formation suggests a more humid phase in the MIS3 period. Alluvial

Please cite this article in press as: Brunetto, E., et al., Analysis of the interaction between neotectonic and surface processes in a low-land intracratonic setting of South America, Quaternary International (2016), http://dx.doi.org/10.1016/j.quaint.2016.06.018

and paludal lenticular facies were also reported from the upper part of the Carcarañá Formation where intraclasts of fine-coarse pebbles are supported in an internally laminated coarse sandy matrix (Kröhling, 1999). These facies were interpreted as localized infilling of ≈50–100 m wide fluvial channels (Fig. 4D).

The Tezanos Pinto Formation is overlying the Carcarañá Formation in erosive unconformity in the southern part of the SGEB. Furthermore, this unit overlies unconformably over the Palo Negro Formation in the northern area of the SGEB (Fig. 4A,B). The Tezanos Pinto unit, formally defined by Iriondo (1987), represents the primary Last Glacial Maximum (LGM) loess, the main component of the Late Quaternary sequences of North Pampa plain, masking the previous landscape (Iriondo and Kröhling, 2007). It is a 2–6 m thick unit comprising a well-sorted light brown, massive and porous silty loam deposit. Secondary structures are represented by burrows, fissures, $CaCO_3$ rhizoliths and concretions. Locally the loess has been fluvial reworked or evolved under non-permanent swamp conditions. TL and OSL datings of the unit indicate an age from ca. 32 to 9 ka. B.P., with its maximum development between 24 and 18 ka. B.P. (Kröhling, 1998, 1999; Kröhling and Iriondo, 2003; Table 1).

The lower member of the LGM loess unit contains a series of laminated structures with well-defined sub-horizontal decimetric to milimetric sorted components of coarse silt, fine silt and clay layers. Such structures reveal some form of water sorting (Kröhling, 1999; Kemp et al., 2004). Facies analysis indicates an environment of low energy, typical of ephemeral ponds and non-permanent waterlogged areas. In the Tortugas quarry section (Fig. 2) a similarly interpreted facies was reported as part of the basal member of the Tezanos Pinto Formation (Fig. 4D) (Kröhling, 1998). But new geochronological data obtained from the same site (Kemp et al., 2004) allows us to think that the deposits of low-energy flows could mostly correspond to the alluvial facies of the Carcarañá Formation. They accumulated during MIS3 (ca. 52–69 ka. B.P.; Table 1), unconformably overlying the truncated paleosol on top of the Ceres/Palo Negro Formation. In that case, only a more restricted part of the stratigraphic column (1–2 m thick) of the Tortugas profile would correspond to the lower member of the Tezanos Pinto Formation (ca. 23 ka. B.P.; Kemp et al., 2004; Table 1). The upper member of the Tezanos Pinto Formation is represented by a primary loess unit (TL and OSL dates ca. 9–8 ka. B.P. near the top; Kröhling, 1999; Table 1), containing numerous bioturbation macrostructures. The loess accumulation covered the fluvial belts developed during the MIS3 and also structural landforms (scarps, tectonic depressions) of the region. The upper member loess forms the parent material of a truncated argillic buried soil developed during the Holocene *Optimum Climaticum*. The San Guillermo Formation (Iriondo, 1987) generally forms the top of the sedimentary sequence in the region. It was derived from the deflation and redeposition of A horizon material from the Holocene soil, with OSL ages of 1–2 ka. B.P. (Kröhling, 1999; Kemp et al., 2004; Fig. 4B; Table 1).

In summary, the lacustrine deposits of Palo Negro/Ceres Formation and the alluvial facies of Carcarañá Formation are good geomorphic markers of recent deformation. Loess composing Tezanos Pinto and San Guillermo Formations has implications for the lithologic control on erosion during the last time.

4. Materials and methods

A geomorphologic evolution model was established by assuming the existence of a topographically flat palaeosurface (slope <0.02°) that evolved into a low slope surface with ENE and NE slope directions (Figs. 3B and 5). The initial flat surface was considered as a geomorphic marker of a pre-deformation condition that evolved into the contemporary tilted and disrupted surface by neotectonic deformation. The older flat topography can be inferred from a regional layer interpreted as ephemeral ponds and shallow lacustrine deposits (Ceres/Palo Negro Formations), dated to ca. 67–178 ka. B.P. (Kemp et al., 2004; Brunetto et al., 2010). The assumption that this surface existed is based on the preservation of a parallel-pattern stream system (channels of 200 m wide and 0.20 m deep) (Fig. 5). Taking into consideration the present stratigraphic knowledge, we associate this facies of laminated silts to the low-energy fluvial deposits (Carcarañá Formation; Fig. 4C–D) that appear in the record of the region, overlying the Ceres/Palo Negro Formations. We interpret these deposits, dated to 52–69 ka. B.P. (Kröhling, 1999; Kemp et al., 2004), constitutes the sedimentary record generated by the parallel-pattern stream system. The sequence Ceres/Palo Negro Formations – Carcarañá Formation can be associated to the pre-deformation reference palaeosurface (Fig. 3B).

A new DEM was achieved for restoring an initial non-deformed topography affected by low fluvial incision as suggested by Burbank and Anderson (2001) and Pelletier (2008). This low-elevation DEM provided the input for the numerical implementation of an erosion code that integrates: (i) diffusion by sheet wash-driven erosion, (ii) incision by fluvial channels, and (iii) surface uplift.

The low-elevation DEM was obtained by carrying out the following steps:

a) Level contours were computed from a SRTM-90m DEM, at 1 m equidistance. b) Sharp inflexions in contours that represent the fluvial valley incisions were removed; c) the elevations of the ground were recalculated with the objective of reducing the slopes in the scarps. For that, a calculator of attributes in a QGIS database was used considering the slope modal values in order to represent the flatter areas of the region (0.02°); d) a simplification of the model was achieved by assuming that the faults respond to a purely reverse displacement mechanism along NNW-SSE and NW–SE fault planes (Brunetto, 2008). In small areas where the fault trends deviate, a rotation was performed in some segments of the level contours, so that they were oriented perpendicularly to the palaeostream directions.

The landscape evolution model is an erosion code that combines the stream power law-advection equation associated with a spatially distributed uplift function and the hillslope diffusion equation (Kaus and Castelltort, 2013). The combined equations were:

$$\frac{\partial h}{\partial t} = -KA^m S^n + U + D\nabla^2 h$$

where K is the erodability coefficient, A is the up-stream drainage area, m n are exponents of stream power, S is the local slope ($\partial h/\partial x$), U is the uplift rate and D the diffusion coefficient.

The erosion code implemented in Matlab by the authors includes four algorithms. The main code *landscape_evolution*, adapted for the geological features of our study area, calls three subroutines *stream_flow_D8*, *StreamPowerlaw* and *Diffusion2D_constant_implicit* (Kaus and Castelltort, 2013).

The numerical modelling of the stream power law implemented by the authors was based on Braun and Willett algorithm (2013) using an efficient and stable first-order finite difference scheme with Newton-Rhapson iterations for n > 1. The streamflow and drainage area is computed according to the D8 routine (O'Callaghan and Mark, 1984) with outflow boundary condition (baselevel nodes) at the bottom and symmetrical boundary conditions. The 2D hillslope diffusion equation was added and solved (Kaus and Castelltort, 2013) by the implicit finite difference method with

Please cite this article in press as: Brunetto, E., et al., Analysis of the interaction between neotectonic and surface processes in a low-land intracratonic setting of South America, Quaternary International (2016), http://dx.doi.org/10.1016/j.quaint.2016.06.018

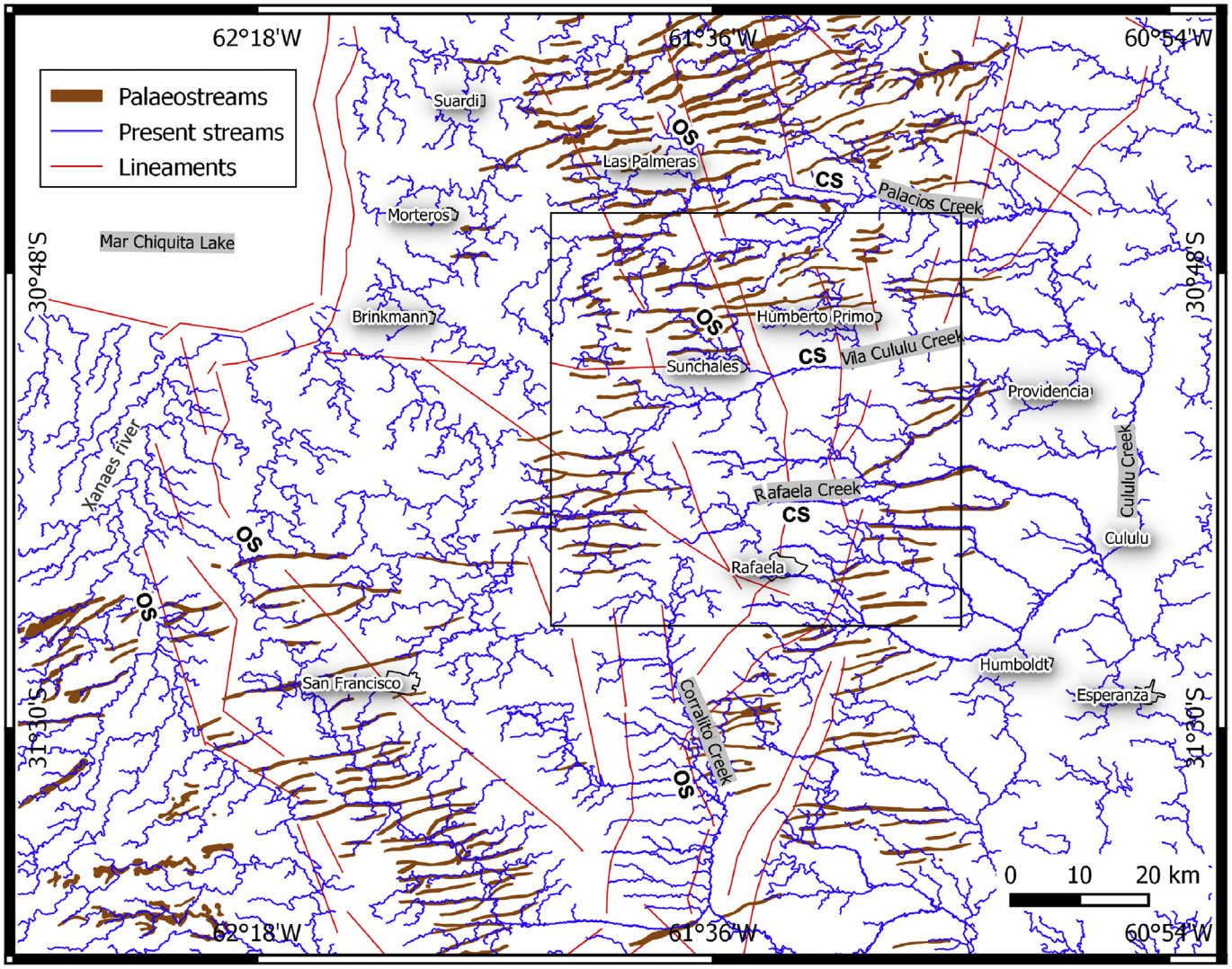

Fig. 5. ENE-trending palaeochannels with parallel drainage pattern (brown) and the superimposed present drainage network (blue). The black quadrate corresponds to the modelled area of Fig. 9. Vila Cululú and Rafaela creeks are consequent streams (CS). Corralito creek, Segundo river and other smaller streams are obsequent streams (OS). (For interpretation of the references to colour in this figure legend, the reader is referred to the web version of this article.)

Dirichlet boundary condition (constant top and bottom elevation) and Neumann boundary condition (left and right boundaries to flux free).

Although the SPL is widely used in the community and has been implemented in various landscape evolution models (LEMs) (Crave and Davy, 2001; Tucker et al., 2001; Braun and Willett, 2013), the values of K, m, n and D remain poorly constrained. These parameters depend on numerous factors and cannot easily be measured from direct field observations (Croissant and Braun, 2014). For this reason, the estimation of the model parameters was achieved by applying the inversion method (Croissant and Braun, 2014). The best-fit between the numerical solution (calculated topography) and the measured topography (simulated by using a DEM) was undertaken. At first, the values of m, n and U were fixed to deduce K.

The uplift function (Appendix 1) was assumed to be spatially variable non-linearly, growing from East to West and from North to South along a cell grid up to reach the maximum heights of the main scarp. From these positions, the uplift was considered to be constant southwestwards (constant in x and y). The maximum uplift rate used in the matrix was derived from the best-fit obtained in the numerical solution, when the maximum heights measured in the SRTM-90m were attained. This last step was considered as representative of the present-day relief. The approach was tested by comparison of the elevation cumulative frequency distributions of the calculated and measured topography. From the maximum value as constrain, the faster spatial variations of the uplift rate were estimated and distributed along the steepest scarp locations in the matrix (Appendix 1).

The ratio $\theta = m/n$ is called the concavity as its value is mostly constrained by the concavity of river profiles. The selection of m and n coefficients was based on the expectation that concavity indices of steady-state channels should fall into a relatively restricted range ($0.4 \leq \theta \leq 0.6$) (Kirby and Whipple, 2012).

In order to assess the discrepancies between theoretical and measured elevations generated by incision, swath longitudinal profiles along the main incised fluvial channels were computed for both the final calculated DEM and the SRTM-90m DEM. ΔH is the difference between the maximum and minimum elevations in each swath point. These were considered as a measurement of the fluvial incision. Geochronological ages of the sediments assumed

Please cite this article in press as: Brunetto, E., et al., Analysis of the interaction between neotectonic and surface processes in a low-land intracratonic setting of South America, Quaternary International (2016), http://dx.doi.org/10.1016/j.quaint.2016.06.018

to be associated to the initial surface were also employed as constraints for the estimation of the model parameters. The incision rate was estimated from the ratio between the maximum ΔH value measured in the fluvial valley from the SRTM-90m DEM, and the total time obtained in the numerical solution of the erosion code.

The geomorphometric processing was performed by GRASS-GIS and QGIS free software.

The elevation data correspond to the headwater area of the Cululú River sub-basin (Salado River Basin), which is entirely situated in the Northern Pampa region (30°45′–31°22′S and 61°10′–61°53′W; Fig. 2). The upper basin and highest headwaters of the Salado system are located in the Eastern Andean Cordillera, 2200 km away towards the NW. The study area is placed in the upland plains that correspond to the eastern limit of the morphostructural SGEB (Fig. 2). The creek named *Vila-Cululú*, a tributary of the Cululú River, was selected for carrying out the numerical assessment. This is a 70 × 70 km area with maximum elevations ca. 108 m.a.s.l. and minimum ca. 60 m.a.s.l. The Vila-Cululú creek is clearly incised into the steeper hillslopes of the flexural scarps that limit the SGEB and the SCB respectively (Fig. 6A).

5. Results

5.1. Drainage analysis

The present Cululú River drainage network simulated from the derived DEM data, displays a dendritic pattern in its upper catchment area formed by low-hierarchy streams. Well-developed fluvial channels of small streams and creeks drain the higher reaches eastwards, into the Salado River channel (Fig. 2). The network pattern is conditioned by a homogenous lithology (loess) and very gentle slopes.

Satellite Images enable the identification of a network of parallel palaeochannels (Fig. 5). This had already been reported in the region (Pasotti, 1974, 1975). The palaeochannels are preserved only locally in the low zones. This observation suggests that low zones are dominated by sedimentation, whereas higher areas were eroded, removing the channel traces. At present, the local low zones are partially occupied by intermittent shallow ponds that are flooded during extremely humid years (Iriondo and Drago, 2004; Brunetto, 2008; Kröhling and Brunetto, 2013). Several of these depressions have a rectangular pattern, which was interpreted to

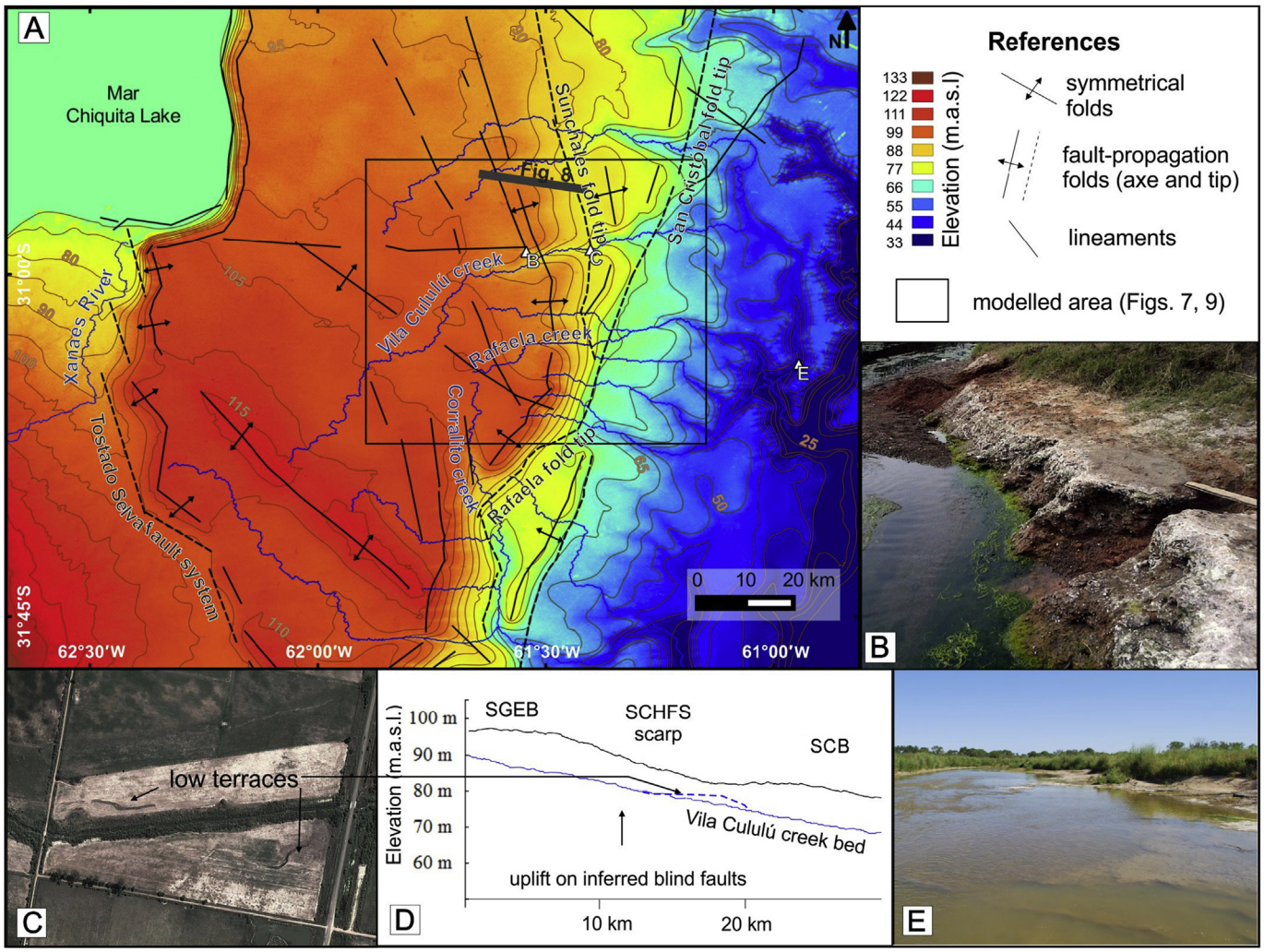

Fig. 6. A) Structural map of the San Guillermo and San Cristobal elevated blocks where the studied region is located. Hills with rectilinear ridges were interpreted as fault-propagation folds on blind faults (Fig. 8). Flexural scarps are the steeper hillslopes. Toeslopes correspond to the fault-tip projections on surface (fold tips). The black quadrate indicates the modelled area of Figs. 7 and 9. B) Outcrop of the Palo Negro Formation near Sunchales city (Fig. 4E and point B in 6A: 30°57′2″S; 61°32′33″W). C–D) Localized terraces (point C in 6A: 30°56′47″S, 61°24′7.1″W) suggest a change in the base level at the fold tip line area. E) Low rapids formed in the Cululú creek over the Palo Negro Formation substratum (point E in 6A: 31°11′46″S; 60°56′42″W).

Please cite this article in press as: Brunetto, E., et al., Analysis of the interaction between neotectonic and surface processes in a low-land intracratonic setting of South America, Quaternary International (2016), http://dx.doi.org/10.1016/j.quaint.2016.06.018

be generated by neotectonics (Brunetto, 2008; Kröhling and Brunetto, 2013).

The coexistence of two different superimposed drainage networks (Fig. 5) suggests a change in climatic and/or tectonics conditions during the Late Pleistocene. Furthermore, it is possible to identify different genetic types of the present stream channels due to structural control on the flow dynamics. Low-hierarchy channels constitute obsequent streams that adapted their flow directions to the slopes modified by displacements on faults (Figs. 5 and 6A). For example, ENE palaeostreams shifted to the present SE, SW, and even W flow directions (Fig. 5). The Corralito creek is an example of an obsequent stream (Fig. 6A). The main courses such as Vila-Cululú and Rafaela creeks (Fig. 6A), are consequent, and overcame the uplift of the crustal blocks.

5.2. Tectonic Geomorphology

Surface ruptures cannot be observed in the Chaco-Paraná sedimentary basin. However, numerous stratigraphic and geomorphologic evidences indicate that Late Quaternary deformation has affected the sedimentary cover (Brunetto, 2008; Brunetto et al., 2010). Aligned hills show rectilinear ridges and hillslopes with a dominant NNW-SSE trend and two secondary NW–SE and NNE-SSW trends (Fig. 6A). These rectilinear features displaying a well-defined trend pattern suggest that localised movements on fault planes have perturbed sedimentary layers (Figs. 3B and 7). These low relief surface undulations in the topography can be interpreted by the formation of gentle fault-propagation folds (Fig. 3). Two vertical component magnitude orders of the low relief growing folds can be observed: 10–30 m and 0.50–1.50 m high. Flexural scarps were generated in these steeper forelimbs (Fig. 3C–D). The higher flexural scarps limit the major blocks (Fig. 3B–D). The folds display asymmetrical cross-sections comprising a steeper flank and a nearly flat surface in the other flank. Each flank is around 10 km long (Fig. 3C–D). The upper flat plains corresponding to the regional morphostructures (SGEB and SCB) can be identified by simple statistics. Two modal values of elevations represent the flat upper surfaces of these main blocks (Brunetto et al., 2014).

In the western side of the SGEB, TSFS (Figs. 2 and 6A) displays a higher scarp in the northern cross-section CC' (over 30 m; Fig. 3C) than in the southern cross-section DD' (over 15 m; Fig. 3D). Several smaller hills (1–2 m height) are also present. They can be observed mainly over the upper surfaces of both blocks (Fig. 3). These subtle flexures generated a strong control on flow directions of both poorly channelized streams and small creeks, shifting them sharply relative to the direction of palaeochannels (Fig. 5). The small folds show either asymmetrical or symmetrical cross-sections (Fig. 3C–D).

In the restricted area selected for the erosion modelling, the main structural orientations are NNW-SSE and NNE-SSW trends (Figs. 6A and 7). In the northern zone of the study area the deformation can be interpreted to be partitioned into two faults: Sunchales fault system and San Cristobal fault (Figs. 6A and 7). The steeper steps that form flexural scarps have $\Delta H \approx 13–15$ m (SGEB/Sunchales fault scarp; Fig. 8) and $\Delta H \approx 12–14$ m (SCB/San Cristobal fault scarp), respectively (Fig. 3C). In the southern area, near Rafaela city, these steps join together forming an unique higher scarp (Rafaela fault; Figs. 6A and 7) that displays a $\Delta H \approx 30$ m (Fig. 3D). In some places this reaches up to 40 m. The total height of the scarp in the eastern area of the SGEB can be assumed to be the result of uplift distributed over several successive folds (Fig. 8). According to this interpretation, the uplift developed an increase in the fold crest heights (Fig. 8B). Such growth caused an increase in valley slope of the incised streams on the downstream side of the fold axis, with a lowered slope on the upstream fold flank. For this reason, a well-defined knickzone appears in the longitudinal profiles of the Vila-Cululú stream (Fig. 8A). This slope inflection is localised at around 15 km upstream from the top of the scarp limiting the structural blocks. The Vila-Cululú stream is poorly channelised on the SGEB flat surface upstream from this knickpoint, displaying shallow and diffuse channels. The shallowing of the drainage in the upper domain and the change to a channelised pattern downstream, strongly suggest that the pattern is the effect of surface uplift (Ouchi, 1985). The stretches of the stream valley that display higher incision are positioned along the axis of the several folded surfaces, indicating that uplift is likely to be concentrated in a group of subsurface fault zones. In these sectors, low terraces appear partially preserved inside the stream valley (Fig. 6C). Such terraces (<1 m high) are preferentially positioned at the base of the scarps, suggesting a line where the slope changes significantly, corresponding to surface projection of a propagating

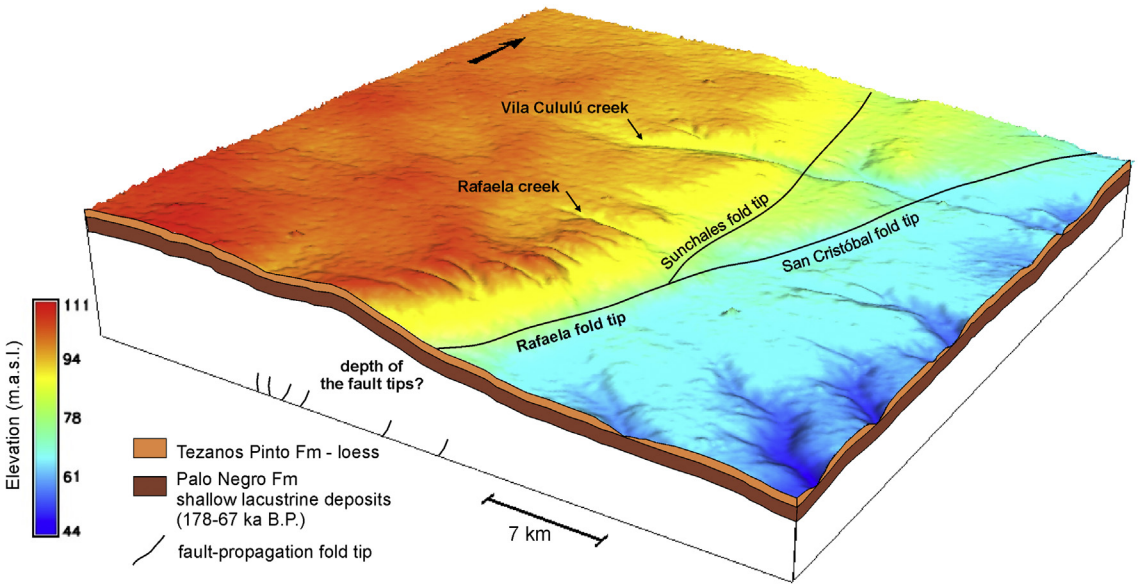

Fig. 7. 3D SRTM-90m DEM (7 × 7 filtered) of the modelled area achieved by NVIZ module in GRASS-GIS software, showing the geological interpretation.

Please cite this article in press as: Brunetto, E., et al., Analysis of the interaction between neotectonic and surface processes in a low-land intracratonic setting of South America, Quaternary International (2016), http://dx.doi.org/10.1016/j.quaint.2016.06.018

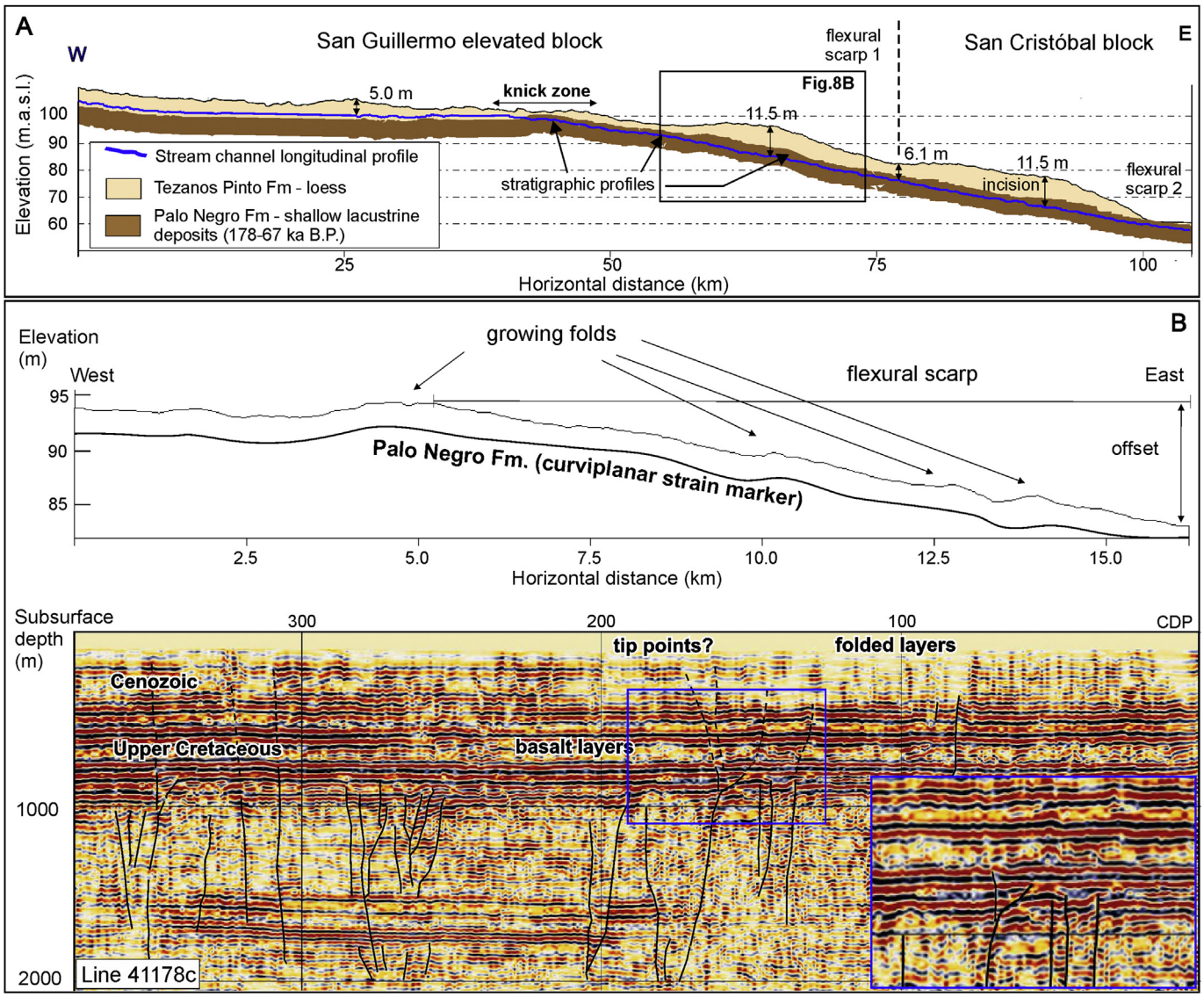

Fig. 8. A) Vila Cululú valley longitudinal profile through the eastern flexural scarps based on SRTM-90m DEM data. The stream channel cuts Palo Negro Formation in the knickzone. The valley incision is higher in the growing fold areas. B) Interpretation of the 41178c seismic line (YPF). See location in Fig. 6A (modified from Brunetto, 2008).

fold tip (Figs. 6A and 7). The presence of localized terraces marks a change in the base level of the stream (Fig. 6D). This can be interpreted as an evidence of active surface faulting (Ouchi, 1985). Other causes cannot be dismissed, such as human activity. However, the presence of these terraces placed exactly at the toeslope is quite suggestive.

The evidence for Quaternary deformation can be time-constrained by the geomorphic horizontal markers linked to the shallow lacustrine and fluvial palaeoenvironments: (i) a regional low-land landscape characterised by shallow lakes and ponds (178–67 ka. B.P.), and (ii) a parallel stream system (tentatively 52–69 ka. B.P.) that can be associated to a regional structural slope with a low constant gradient (Fig. 3B). Horizontal markers observed in outcrops located on the scarps suggest that the deformation began after than the sedimentation of the Palo Negro Formation ended (Figs. 6B and 8A). This interpretation indicates that a palaeosurface characterised by net accumulation was progressively shifting into the present erosion surface, affected by river valley incision. It is possible to infer that the main deformation was concentrated by displacements on faults that developed the gentle folding of the sedimentary cover and generated higher and steeper flexural scarps. If an average age of 100 ka., based on the available geochronological data, is considered as constraint for the beginning of the deformation, then uplift rates post Palo Negro Formation deposition can be estimated between 0.12 and 0.15 mm/yr in the Sunchales fault system (SFS) and San Cristobal fault system (SCFS), located in the northern study area, and 0.3–0.4 mm/yr in the Rafaela fault, in the southern area (Figs. 2, 3C–D, 6A and 7; Table 2).

5.2.1. Interpretation of the structural style

Since just a few historical earthquakes without geophysical and geological analyses have been reported in the region, it is not possible to say what the mechanism of the deformation is. There are not elements for interpreting if the deformation involves large seismic events, or slow and aseismic displacements on faults in the study area (Brunetto, 2008). Only an averaged deformation over a Late Quaternary span of time (1×10^5 yr) can be interpreted from the available data. In recent works, deformation is suggested to occur on faults that can be inferred in the subsurface from seismic

Please cite this article in press as: Brunetto, E., et al., Analysis of the interaction between neotectonic and surface processes in a low-land intracratonic setting of South America, Quaternary International (2016), http://dx.doi.org/10.1016/j.quaint.2016.06.018

Table 2
Uplift and incision estimated from DEM data. 2.1: uplift rates estimated on the flexural scarps located in the eastern margin of the main blocks, for 65 and 100 ka. B.P. 2.2: maximum fluvial incision rates estimated on the maximum river valley depths, located in the eastern margin of the main blocks, for 65 and 100 ka. B.P.

	Age (ka)	Sunchales fault		San Cristobal fault		Rafaela fault	
		ΔH_1	ΔH_2	ΔH_1	ΔH_2	ΔH_1	ΔH_2
Integrated scarp height (m)		13	15	12	14	30	40
Uplift rates max. age 1 (mm/yr)	65	0.20	0.23	0.18	0.22	0.46	0.62
Uplift rates max. age 2 (mm/yr)	100	0.13	0.15	0.12	0.14	0.30	0.40
	Age (ka)	SGEB eastern scarp		SCB eastern scarp		SGEB eastern scarp	
		ΔH_1	ΔH_2	ΔH_1	ΔH_2	ΔH_1	ΔH_2
Integrated scarp height (m)		12	14	10	12	15	18
Incision rates max. age 1 (mm/yr)	65	0.18	0.22	0.15	0.18	0.23	0.28
Incision rates max. age 2 (mm/yr)	100	0.12	0.14	0.10	0.12	0.15	0.18

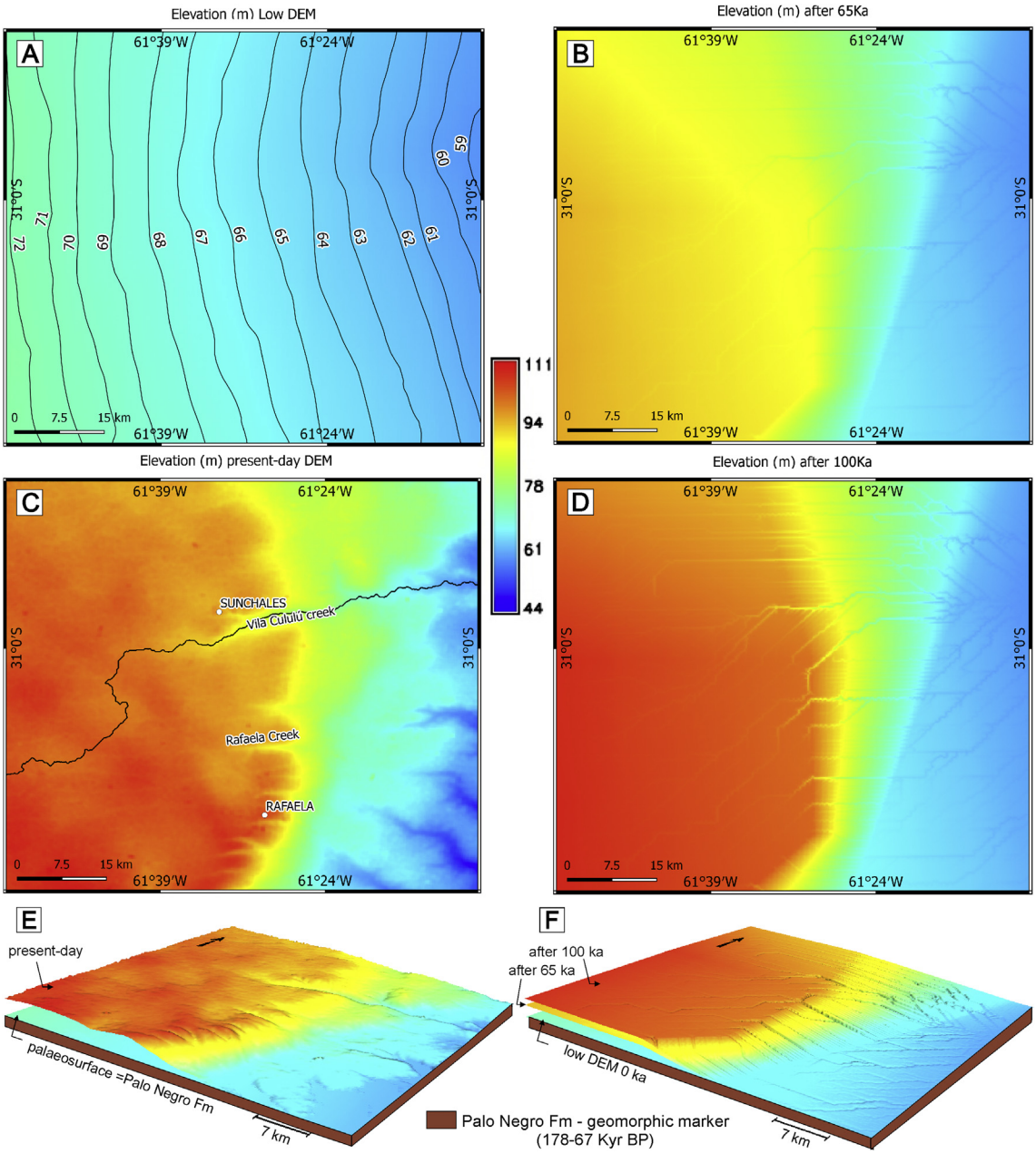

Fig. 9. A) Simulated low-DEM that represents a pre-deformation surface affected by low fluvial incision (To). B) Topography calculated from numerical modelling, after 65 ka. C) The SRTM-90m DEM (7 × 7 filtered) representing the present relief and topography. D) Topography calculated from numerical modelling, after 100 ka. E) 3D SRTM-90m DEM (present day). F) 3D topography representing the landscape evolution model.

Please cite this article in press as: Brunetto, E., et al., Analysis of the interaction between neotectonic and surface processes in a low-land intracratonic setting of South America, Quaternary International (2016), http://dx.doi.org/10.1016/j.quaint.2016.06.018

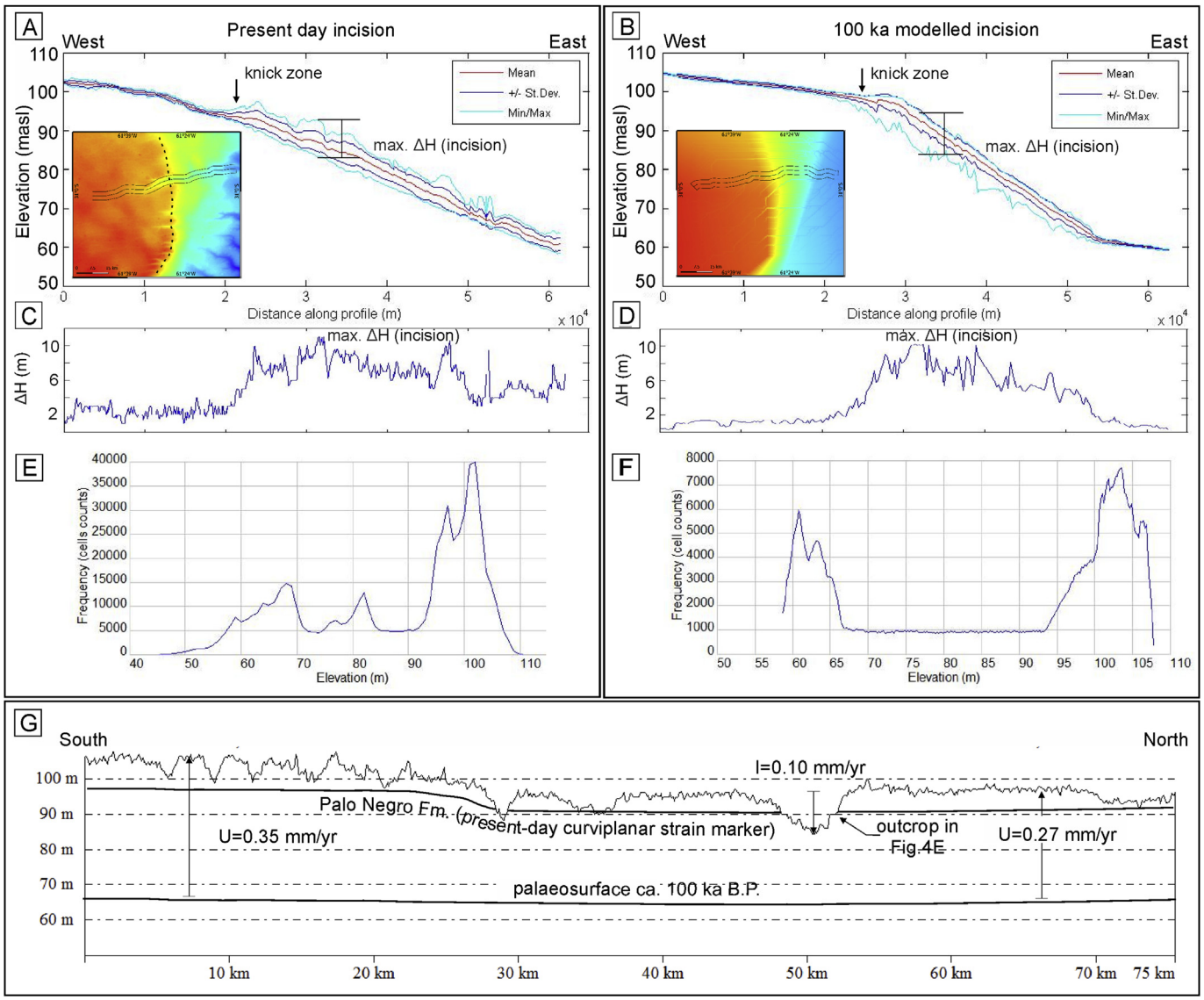

Fig. 10. The best-fit between the measured topography (A: simulated by means a SRTM-90m DEM) and the numerical solution (B: calculated topography) was approached by comparison of the swath stream longitudinal profiles. The constrains for testing the approach were the fluvial incision in the main stream and the final elevation distributions. Fluvial incision was represented by the elevation difference (ΔH) in the fluvial valley from swath stream longitudinal profiles of: C) measured topography; D) numerical solution. Final elevation distributions were represented by frequency histograms of: E) measured topography; F) numerical solution. G) Tectonic Geomorphology interpretation (dashed line in Fig. 10A).

sections (Brunetto, 2008; Brunetto et al., 2010) (Fig. 8B). They were interpreted as old normal faults bounding graben and half-graben structures that were generated during the Mesozoic crustal stretching of the Gondwana supercontinent (Chebli et al., 1999; Webster et al., 2004; Brunetto et al., 2010). The presence of local Cretaceous depocenters limited by high-angle normal faults was also interpreted in several places of the Northern Pampa region from gravimetric data (Webster et al., 2004; Gimenez et al., 2011; Brunetto and Gimenez, 2012). Therefore, the combination of indirect manifestations of tectonic deformation in surface and the presence of Cretaceous faults affecting the sedimentary fill of the Chaco-Paraná basin suggest that recent faulting occurs by the inversion of pre-existing zones of weakness in the upper crust. A general W–E maximum compressive stress direction can be inferred from geodetic data for the studied area. Regionally, relative displacement velocities between GNSS permanent stations (baselines) suggest a compressive/transpressive regime and shortening velocities of around 2 mm/yr in the centre of the Rio de la Plata Craton (Sobrero and Brunetto, 2015). The residual velocity field shows a resultant shortening axe with an ESE trend (102°E), which differs slightly from the convergence vector between the Nazca and South American plates (ENE/78°E). The interpreted stress field strongly suggests the influence of far-field forces generated in the plate margins. The dynamics interpreted from the geophysical and geodetic data can explain a reverse kinematics of NNW-SSE-trended structures, roughly perpendicular respect to the regional direction of maximum compressive stress. Dominant strike-slip displacements can be related to the reactivation of NW–SE ancient intraplate transverse accommodation zones generated during the opening of the Atlantic Ocean (Jacques, 2003), being responsible of the geometry of NW-SE-trended symmetrical folds.

5.3. Fluvial incision model

he restored palaeosurface topography associated with the pre-deformation lowlands (t = 0, slope ≤ 0.02°) resulted in elevations that range between 59 and 73 m.a.s.l. (Fig. 9A). The current surface of the study area is located at elevations between 60

Please cite this article in press as: Brunetto, E., et al., Analysis of the interaction between neotectonic and surface processes in a low-land intracratonic setting of South America, Quaternary International (2016), http://dx.doi.org/10.1016/j.quaint.2016.06.018

and 108 m.a.s.l. (Figs. 9C and 10E). The best-fit that reproduces roughly the present topography from a low-elevation surface (Fig. 10) is obtained from the parameters displayed in Table 3.1. Minimum height differences between surface elevations and the incisions between the calculated and measured models are reached when the main stream displays maximum incision values of ca. 9–12 m (Fig. 10C, D; Table 3.2). Differences in the drainage pattern between the modelled and present topography appears to be because of the real orientation of slopes and that structural controls on the drainage respond to a more complex pattern. The erosion model cannot reproduce exactly the effect on the ground from oblique displacements on the faults or from non-uniform distribution of the uplift forces. This is a model that attempts to estimate the vertical component of the tectonic uplift from oblique slips. There is no net compressive tectonics, as it was interpreted by Brunetto (2012), Sobrero and Brunetto (2015). However, the final modelled surface resembles acceptably the real topography (Fig. 9). The time required to reproduce the modern landscape using the best numerical approach was 100 ka (Fig. 9D–F). It is comprised between the range of the geochronological data obtained in the Palo Negro Formation (67–178 ka.). A maximum uplift rate of 0.35 mm/yr was required to achieve the present highest elevations (Table 3.1). Previous estimations on Tostado-Selva fault (western SGEB) suggest uplift rates ranging in 0.27–0.4 mm/yr (Brunetto, 2008; Costa et al., 2014). Maximum incision rates of 0.10–0.14 mm/yr can be estimated over swath profiles when considering a maximum ΔH of ca. 10–14 m for the present incised valley of Vila-Cululú stream, excavated on the Late Pleistocene sediments during a span of time of 100 ka. (Table 2). Further south, in Rafaela fault area, the estimated incision rates result to be higher than in the Sunchales scarp, at 0.15–0.18 mm/yr. If the total time used in the modelling is 65 ka. (estimated age of the palaeostreams), maximum elevations observed in the upper surface of the SGEB cannot be reproduced (Fig. 9B).

Table 3.1
Values of the empirically estimated parameters for the erosion numerical model. Parameters for the best-fit.

Parameters of the model			
Erodability coefficient range	*K*	5×10^{-6}–6×10^{-6}	
Diffusion coefficient range	*D*	1×10^{-9}–6×10^{-9}	mm^2/sec
Stream power exponent	m	0.5	
Stream power exponent	n	1.0	
Max. uplift rate (range)	U	0.27–0.35	mm/yr
Time steps	nt	100	ka

Table 3.2
Values of the empirically estimated parameters for the erosion numerical model. Different *K* and *D* coefficients tested and their influence on maximum fluvial incision.

Parameter estimation		
K	*D* (mm^2/sec)	Maximum incision (m)
1.00E-06	5.00E-08	1.5
2.00E-06	1.00E-08	3.7
1.00E-06	1.50E-08	3.9
5.00E-06	1.00E-08	8.5
6.00E-06	6.00E-09	9.1
5.00E-06	3.00E-09	9.3
5.00E-06	1.00E-09	11.2
6.00E-06	5.00E-09	11.7
7.00E-06	1.00E-09	12.5
1.00E-05	1.00E-09	14.3
6.00E-06	1.00E-09	14.3

The comparison of the estimated incision rate with the uplift rates, which were obtained either from the structural estimations or from the landscape evolution model (Table 2), suggests that the system is not adjusted. The general model records the development of the Rafaela scarp. The longitudinal profile of the Corralito creek crossing the Rafaela scarp displays localised increases in slope which suggests that the channel profile is not adjusted. However, both in the SGEB and SCB scarps, uplift and incision rates seem to be closer to equilibrium and it is not possible to detect significant changes in slope along the longitudinal profile (Figs. 8A and 10A). This is probably due to where deformation is partitioned between both faults and the uplift is distributed in a wider space linked to more than one axis of uplift. This causes uplift rates on individual faults to be lower than if the uplift were concentrated on a specific fault system. Such observations seem to indicate that the stream power of the Vila-Cululú is sufficient so that the stream can cross the growing fold and be consequent with its original slope direction. In contrast, the stream power of the Corralito creek is insufficient to allow the stream to cut the crest of the fold and thus it is forced to bend to the south (Fig. 6A).

6. Discussion

This is a first approach addressed to test the magnitude order for the interaction between surface processes and tectonics in intracratonic settings comprising the Chaco-Pampean region during the Upper Quaternary. As little background concerned about quantitative models is available for these settings, an empirical approach for the estimations of the parameters involved in an erosion code based on the SPL, seems to be a good attempt. The feasibility to apply that procedure is justified in the fact that the stratigraphy is simple, reasonably known and provides sound geometrical and chronological markers for the beginning of a cycle of landscape evolution. The model assumes that differential uplift exerts an active control on the geomorphic processes during the Late Pleistocene/Holocene. Shallow lacustrine sediments in steeper slopes along the scarps are robust evidence for supporting this assumption. Widespread wetlands would not be possible to be located in such scarps, where generalised incision is happening at present.

Firstly, the regional uplift rate value (0.35 mm/yr) obtained for the best-fit of the model is higher than uplift rates (0.25–0.1 mm/yr) reported in low uplift rate settings (Lagarde et al., 2000, 2003; Quigley et al., 2006). The intraplate uplift rates obtained for the Late Pleistocene/Holocene (1×10^5 yr) scale are noticeable higher than rates of averaged long-term deformation (Cenozoic scale) (Hillis et al., 2008). This fact is attributed to the episodic character of the deformation, where short-time events are separated by long periods of quiescence (Crone et al., 1997, 2003). The high value obtained can be considered more broadly in the context of the Pampean foreland dynamics, where the Nazca Plate flat-slab subduction drives the deformation far away from the plate margin (Ramos et al., 2002). Additionally, maximum uplift inferred for the restricted study area is compatible with 2 mm/yr far-field shortening estimated for the region. Even more, if it is considered that part of the uplift can be produced by isostatic loads due to flexure by tectonic load in the easternmost Pampean ranges (Dávila et al., 2010). The last forces operate in a longer topography wavelength.

Otherwise, the empiric value for *K* (5×10^{-6}–6×10^{-6} yr^{-1}, Table 3) is lower than the value normally used in studies of mountainous landscapes (1×10^{-5}–1×10^{-4} yr^{-1}) (Whipple and Tucker, 1999; Croissant and Braun, 2014). Despite the fact that the unconsolidated sedimentary substratum is expected to be more susceptible to erosion, low *K* values suggest that the extremely low

Please cite this article in press as: Brunetto, E., et al., Analysis of the interaction between neotectonic and surface processes in a low-land intracratonic setting of South America, Quaternary International (2016), http://dx.doi.org/10.1016/j.quaint.2016.06.018

slopes exert a larger influence on the stream power. The slope magnitude appears to be the more significant factor controlling erosion in this lowland landscape. Along most of the longitudinal profile, the Vila-Cululú active fluvial channel is a non-consolidated sediment-floored stream (loessic substratum), with clearly weaker resistance than any bedrock channel substratum, a case more widely studied. For this reason the knickzone is long (several kilometres) and it should be expected that erosion occurs by slope replacement rather than by scarp retreat (Seidl and Dietrich, 1992; Ouchi, 1985). However, the outcrops of the Palo Negro Formation at the river channel are probably affecting its slope. The sedimentary characteristics of the Palo Negro with respect to the overlying loess formation generate a more resistant stratum, probably contributing to a low *K* value. Post-depositional processes have affected this formation and have conditioned it with a moderate degree of consolidation. Small scale erosional features appear in several places of the Vila-Cululú channel forming the observed rapids. Alluvial bedforms are not frequent inside the fluvial valley, whereas low terraces appear only in localised areas. These erosional features supply additional evidence supporting the interpretation that the dynamics of erosion of the analysed fluvial channels is detachment-limited.

The values of the selected *m* y *n* exponents, which make sure the concavity index to be inside the range established in literature ($0.4 \leq \theta \leq 0.6$), should be tested through a more specific analysis. This choice supposes the channel is in steady state equilibrium, situation that does not appears to be occurring at present. The transient response of channels to tectonic forcing can be reflected in the evidence of subtle changes in the base level that provoked the formation of low terraces near the fold tip. The general observation that the concavity index (θ) is relatively insensitive to differences in rock uplift rate, climate or substrate lithology at steady-state (Wobus et al., 2006; Kirby and Whipple, 2012), makes us to think the adopted criterion can be reasonably for this first modelling in a lowland region. The practical determination of the concavity index (θ) and channel steepness index (*ks*) can be accomplished from analysis of slope-area. The study of this scaling relationship could be a key to understand the spatial and temporal history of rock uplift and for distinguishing the complex influence of substrate properties (the Palo Negro Formation in our case), sediment load characteristics, and discharges patterns (Kirby and Whipple, 2012).

The response time for the channel adjustment is difficult to estimate because of the detailed sequence of changes in the discharges and how they were distributed over time is not known. From studies developed in the neighboring region of Argentine Mesopotamia it is proposed that the highest discharges happened during interglacial periods in the distal area of the Paraná River basin (Brunetto et al., 2015b). The Northern Pampa region is also part of the lower basin of the Paraná River, therefore it is reasonable to think that the highest incision rates also occurred in these periods. Otherwise, the effect of lower discharges affecting to the erosion rate during the last glacial stage could have been partially compensated for the increase in the slopes due to a remarkable base level drop. The Salado-Paraná River system is the base level of the Cululú River. This displays terraces that evidence base level changes (Kröhling and Brunetto, 2013). A 150 m drop of the sea level has been estimated for the LGM stage (Guilderson et al., 2000; Kaiser and Lamy, 2010).

The comparison between the incision and uplift rates suggest that the landscape is not in equilibrium (Fig. 10G). Besides, their variations along the different longitudinal profiles indicates that the approximation to an equilibrium state is spatially variable. The adjustment seems to be faster in places where the deformation is distributed in several structures such as the SGEB/Sunchales fault and SCB scarps, e.g. near to Sunchales city (Table 2). In higher scarps like in Rafaela fault, the transient response appears to be longer, and the streams tend to adjust their channels by hydraulic parameters (Schumm, 1986).

Finally, changes for the diffusion coefficient *D* seem to affect largely the magnitude of the denudation. An increase of one magnitude order in *D* reduces exponentially the incision (Table 3.2). In our case, a good fit is attained by using ostensibly lower values (3.2×10^{-4}–1.9×10^{-3} cm^2/yr) than presented in tectonically active landscapes (>0.03 cm^2/yr) (Wallace, 1978; Bucknam and Anderson, 1979; Nash, 1984; Pelletier, 2008). Given that diffusion varies spatially according to climate, vegetation, soil texture and others parameters, a frequent criticism is that we do not know the value of *D* for a given location with any precision. But, it is still important to study hillslope evolution even if the absolute rates cannot be precisely determined (Pelletier, 2008), mainly in poorly known intracratonic areas. So that, a more specific analysis should be carried out in order to understand the impact of diffusion on the global erosion for lowland environments. Particularly, the calculation of the mass balance and sedimentary flux on hillslopes could be yielded trough field experiments (Burbank and Anderson, 2001; Pelletier, 2008); these are in progress for the study area. Incidence of short-term human activities over the intermediate time-scale surface processes is also to be analysed.

The rapid evolution of the landscape in an intracratonic setting that has been inferred from the structural, stratigraphic and geomorphological modelling raises several questions. Sedimentary flux or discharge fluctuations are not the only factors controlling cyclically the accumulation and reworking of the sedimentary record. Changes in the base level of fluvial systems due to differential rock uplift or induced uplift by other endogenous processes such as asthenospheric fluxes (dynamic topography) or flexural deformation by subcortical loads can also provoke fluvial incision and controls in sedimentation. The analysis of the interplay between endogenous and exogenous forcing when modelling landscapes can also be applied by using the assumptions for the modelling of mountain ranges and more tectonically active erosional landscapes (Kirby and Whipple, 2012). For this, a large change in scale should be taken into consideration for analysing the processes that control incision of rivers into bedrock in lowland environments (Burbank and Anderson, 2001).

But a crucial question remains, why does not rapid evolution of the landscape from tectonic forcing produce a long-term accumulated relief along the main fault systems? At first, intensive measurements of erosion rates could be achieved in order to understand how the forces lowering the topography operate. Otherwise, a conceptual model for intracontinental earthquakes has been proposed (Liu et al., 2011). In this, slow tectonic loading in midcontinents is expected to be accommodated collectively by a complex system of interacting faults, resulting in an episodic and spatially migrating pattern of deformation. This model would explain the absence of an accumulated relief over the long-term. The deformation should be expected to be widely distributed amongst a number of fault systems and irregularly through the time. The faults can be active for a short period after long dormancy (Liu et al., 2011). An irregular spatial pattern and out of phase erosion/uplift ratio could explain the absence of a high topography accumulated during the long-term evolution of less active erosional landscapes. This model seems to work for areas with similar characteristics to those of the study area, where deformation is accommodated in a number of structures and highest folds are composed by several smaller folds. Where deformation is slow, erosion by combined diffusion and incision keeps elevations of the landscape close to an equilibrium. Prolonged periods of dominant subsidence (initial stage of the geological model of this work)

Please cite this article in press as: Brunetto, E., et al., Analysis of the interaction between neotectonic and surface processes in a low-land intracratonic setting of South America, Quaternary International (2016), http://dx.doi.org/10.1016/j.quaint.2016.06.018

probably alternate with periods characterised by faster tectonics and uplift (Armitage and Allen, 2010).

7. Conclusions

A geomorphological modelling, stratigraphically constrained and based on the stream power law, which integrates uplift, fluvial incision, and diffusion, is possible to be applied in lowland landscapes. The Northern Pampa region example is a preliminary approach in order to understand the magnitude order of the geomorphic processes controlling the landscape evolution.

An empirical selection of the parameters for the model suggests that a large scale change in magnitude of the processes modelling the landscape should be expected respect to mountain erosional environments. E.g. the empiric value for erodability coefficient K is noticeably lower than the value normally used in studies of mountainous landscapes (5×10^{-6}–6×10^{-6} yr^{-1} vs. $\approx 1 \times 10^{-4}$). Also the diffusion coefficient D values appears to be largely lower (3×10^{-4}–1.9×10^{-3} cm^2/yr) than presented in tectonically active landscapes (>0.03 cm^2/yr). The extremely low slopes can be a higher control than lithology over these parameters.

Uplift rates can be higher (up to 0.35 mm/yr) than is generally expected in low uplift rate settings (0.1–0.25 mm/yr). As a consequence a rapid evolution of the landscape for the Late Pleistocene/Holocene (over intermediate time scales) can be occurring in some intracratonic regions like the Northern Pampa foreland basin.

Highly dynamic recycling of the sedimentary record combined with episodic and migrating uplift phases could explain the fact that a high topography is not preserved over the long-term in intracratonic settings. Complementary, the deformation could be distributing in a wide network of blind faults that folds the Late Quaternary sedimentary cover.

This first analysis suggests that more spatially concentrated the deformation is, stream transient response (uplift/erosion disequilibrium) appears to be longer.

Acknowledgements

This work was funded by the Project CAI+DO 2012 N° 1.5 – UNL (Universidad Nacional del Litoral) and the Project PCTI-92 (PDTS) Mincyt, Argentina. We are grateful to Eng. E. Alasia (Cooperativa de Provisión de Agua Potable y Otros Servicios Públicos de Sunchales Ltda.) for the active role in the Project. We greatly appreciate the thoughtful comments and review by C. Costa (Argentina) and M. Stokes (UK) on the original manuscript. We are also indebted to the comments and suggestions provided by anonymous reviewers that greatly improved the manuscript.

Appendix A. Supplementary data

Supplementary data related to this article can be found at http://dx.doi.org/10.1016/j.quaint.2016.06.018.

References

Alves, M.C.S., Santos, M.C., Gemael, C., 2003. A velocity field estimation of the Brazilian portion of the SOAM plate. GPS Solutions 7 (3), 186–193.

Armitage, J.J., Allen, P.A., 2010. Cratonic basins and the long-term subsidence history of continental interiors. Journal of the Geological Society, London 167, 61–70. http://dx.doi.org/10.1144/0016-76492009-108.

Assumpção, M., 1992. The regional intraplate stress field in South America. Journal of Geophysical Research 97 (8), 11889–11903.

Assumpção, M., Suarez, G., 1988. Source mechanism of moderate size earthquakes and stress orientation in mid-plate South America. Geophysical Journal 92, 253–267.

Bezerra, F.H.R., Vita-Finzi, C., 2000. How active is a passive margin? Paleoseismicity in northeastern Brazil. Geology 28, 591–594.

Bezerra, F.H.R., Ferreira, J.M., Sousa, M.O.M., 2006. Review of seismicity and Neogene tectonics in Northeastern Brazil. Revista de la Asociación Geológica Argentina 61 (4), 525–535.

Bezerra, F.H.R., Brito Neves, B.B., Corrêa, A.C.B., Barreto, A.M.F., Suguio, K., 2008. Late Pleistocene tectonic-geomorphological development within a passive margin — the Cariatá trough, northeastern Brazil. Geomorphology 97, 555–582.

Blum, M.D., Törnqvist, T.E., 2000. Fluvial responses to climate and sea-level change: a review and look forward. Sedimentology 47 (Suppl. 1), 2–48.

Braun, J., Willett, S.D., 2013. A very efficient O(n), implicit and parallel method to solve the stream power equation governing fluvial incision and landscape evolution. Geomorphology 180–181, 170–179.

Brunetto, E., 2008. Actividad neotectónica en el sector oriental de la cuenca inferior del río Dulce, laguna Mar Chiquita y bloque San Guillermo. Tesis Doctoral. Universidad Nacional de Córdoba, Córdoba, p. 306 (unpublished).

Brunetto, E., 2012. Desplazamientos laterales neógenos en fallas del sur de Entre Ríos, a partir de evidencias estratigráficas, geomorfológicas y datos de GPS. Jornada Abierta de Comunicaciones Científicas del IGEBA. Tectónica de Desplazamiento de Rumbo. Dpto. de Ciencias Geológicas de la UBA, Buenos Aires, abstracts: 6.

Brunetto, E., Iriondo, M., Zamboni, L., Gottardi, M.G., 2010. Quaternary Deformation around the Palo Negro area, Pampa Norte, Argentina. Journal de South American Earth Sciences 29, 627–641.

Brunetto, E., Gimenez, M.E., 2012. Características de la deformación cuaternaria en el centro de la llanura pampeana. In: XV Reunión de Tectónica. San Juan, pp. 36–37.

Brunetto, E., Kröhling, D., Francisconi, C., 2014. La geomorfología de una región representativa de Pampa Norte y sur de la Mesopotamia en el contexto de los procesos endógenos. In: Aportes para el mapeo de áreas de llanura. XIX Congreso Geológico Argentino. Córdoba, 2–6 de junio, p. S13.

Brunetto, E., Kröhling, D., Francisconi, C., Zalazar, C., 2015a. Quantitative Geomorphology applied to the distal Salado del Norte River basin, Argentina. In: Neotectonic and Surface Processes in an Intracratonic Setting. Abstract XIX INQUA Int. Congress (Nagoya, Japan, 2015), p. 11.

Brunetto, E., Ferrero, B., Noriega, J.I., 2015b. Late Pleistocene lithostratigraphy and sequences in the Southwestern Mesopotamia (Argentina): evidences of the Last Interglacial Stage. Journal of South American Earth Sciences 111–128. http://dx.doi.org/10.1016/j.jsames.2014.12.003.

Bucknam, R.C., Anderson, R.E., 1979. Estimation of fault-scarp ages from a scarp-height-slope-angle relationship. Geology 7, 11–14.

Burbank, D.W., Anderson, R.S., 2001. Tectonic Geomorphology. Blackwell Science, Oxford, p. 274.

Carretier, S., Nivière, B., Giamboni, M., Winter, T., 2006. Do river profiles record along stream variations of low uplift rate? Journal of Geophysical Research 111, F02024. http://dx.doi.org/10.1029/2005JF000419.

Chebli, G., Mozetic, M., Rossello, E., Bühler, M., 1999. Cuencas sedimentarias de la llanura Chacopampeana. In: Caminos, R. (Ed.), Geología Argentina. Instituto de Geología y Recursos Minerales, Anales 29(20), pp. 627–644. Buenos Aires.

Costa, C.H., Murillo, V., Sagripanti, G.L., Gardini, C., 2001. Quaternary intraplate deformation in the southeastern Sierras Pampeanas, Argentina. Journal of Seismology 5, 399–409.

Costa, C.H., Massabie, A.C., Sagripanti, G.L., Brunetto, E., Coppolecchia, M., 2014. Neotectónica. In: Martino, R., Guereschi, A. (Eds.), Relatorio del XIX Congreso Geológico Argentino – Geología y Recursos Naturales de la Provincia de Córdoba. Asociación Geológica Argentina, pp. 725–746.

Crave, A., Davy, P., 2001. A stochastic precipiton model for simulating erosion/sedimentation dynamics. Computers & Geosciences 27, 815–827.

Croissant, T., Braun, J., 2014. Constraining the stream power law: a novel approach combining a landscape evolution model and an inversion method. Earth Surface Dynamics 2, 155–166.

Crone, A.J., Machette, M.N., Bowman, J.R., 1997. Episodic nature of earthquake activity in stable continental regions revealed by palaeoseismicity studies of Australian and North American Quaternary faults. Australian Journal of Earth Science 44 (2), 203–214.

Crone, A.J., De Martini, P.M., Machette, M.N., Okumura, K., 2003. Paleoseismicity of aseismic Quaternary faults in Australia-implications for fault behavior in stable continental regions. Bulletin of the Seismological Society of America 93 (5), 1913–1934.

Cunha, F.M.B. da, 1988. Controle tectônico-estrutural na hidrografia na região do Alto Amazonas. In: Congresso Brasileiro de Geologia, 35, Bélem, 1988: Anais Sociedade Brasileira de Geologia, Belém-NO, 5, pp. 2267–2273.

Dávila, F.M., Lithgow-Bertelloni, C., Gimenez, M., 2010. Tectonic and dynamic controls on the topography and subsidence of the Argentine Pampas: the role of the flat slab. Earth and Planetary Science Letters 295, 187–194.

Dávila, F., Lithgow-Bertelloni, C., 2013. Dynamic topography in South America. Journal of South American Earth Sciences 43, 127–144.

De Celles, P.G., Giles, K.A., 1996. Foreland basin systems. Basin Research 8, 105–123.

Font, M., Amorese, D., Lagarde, J.L., 2010. DEM and GIS analysis of the stream gradient index to evaluate effects of tectonics: the Normandy intraplate area (NW France). Geomorphology 119, 172–180.

Gasparini, N.M., Brandon, M.T., 2011. A generalized power law approximation for fluvial incision of bedrock channels. Journal of Geophysical Research 116, F02020. http://dx.doi.org/10.1029/2009JF001655.

Gimenez, M.E., Dávila, F., Astini, R., Martínez, P., 2011. Interpretación gravimétrica y estructura cortical en la cuenca de General Levalle, Provincia de Córdoba, Argentina. Revista Mexicana de Ciencias Geológicas 28 (1), 105–117.

Please cite this article in press as: Brunetto, E., et al., Analysis of the interaction between neotectonic and surface processes in a low-land intracratonic setting of South America, Quaternary International (2016), http://dx.doi.org/10.1016/j.quaint.2016.06.018

Grohmann, C.H., 2004. Morphometric analysis in geographic information systems: applications of free software GRASS and R. Computers & Geosciences 30, 1055–1067.
Grohmann, C.H., 2005. Trend-surface analysis of morphometric parameters: a case study in southeastern Brazil. Computers & Geosciences 31, 1007–1014.
Grohmann, C.H., Riccomini, C., Machado Alves, F., 2007. SRTM-based morphotectonic analysis of the Poc-os de Caldas Alkaline Massif, southeastern Brazil. Computers & Geosciences 33, 10–19.
Guilderson, T., Burckle, L., Hemming, S., 2000. Late Pleistocene sea level variations derived from the Argentine Shelf. Geochemistry, Geophysics, Geosystems 1. http://dx.doi.org/10.1029/2000GC000098, 2000GC000098.
Hillis, R.R., Sandiford, M., Reynolds, S.D., Quigley, M.C., 2008. Present-day stresses, seismicity and Neogene-to-Recent tectonics of Australia's 'passive' margin: intraplate deformation controlled by plate boundary forces. In: Johnson, H., Doré, A.G., Gatliff, R.W., Holdsworth, R., Lundin, E.R., Ritchie, J.D. (Eds.), The Nature and Origin of Compression in Passive Margins, Geological Society, London, Special Publications, 306, pp. 71–90.
Horton, B.K., De Celles, P.G., 1997. The modern foreland basin system adyacent to the Central Andes. Geology 25 (10), 895–898.
Howard, A.D., Kerby, G., 1983. Channel changes in badlands. Geological Society of America Bulletin 94, 739–752.
INPRES, 2010. Listado de terremotos históricos. Catalogo on-line: www.inpres.gov.ar.
Iriondo, M.H., 1987. Geomorfología y Cuaternario de la Provincia de Santa Fe (Argentina). D'Orbignyana, Corrientes 4, 1–54.
Iriondo, M.H., 2010. Geología del Cuaternario en la Argentina. Museo Provincial de Ciencias Naturales Florentino Ameghino, Santa Fe, p. 437.
Iriondo, M., Drago, E., 2004. The headwater hydrographic characteristics of large plains: the Pampa case. Ecohydrology Hydrology 4 (1), 7–16.
Iriondo, M.H., Kröhling, D., 2007. Non-classical types of loess. In: Flemming, B., Hartmann, D. (Eds.), From Particle Size to Sediment Dynamics. Sedimentary Geology, 202(3), pp. 352–368.
Jacques, J.M., 2003. A tectonostratigraphic synthesis of the Sub-Andean basins: inferences on the position of South American intraplate accommodation zones and their control on South Atlantic opening. Journal of the Geological Society, London 160, 703–717.
Jordan, T.A., Allmendinger, R.W., 1986. The Sierras Pampeanas of Argentina: a modern analogue of Rocky Mountain foreland deformation. American Journal of Science 286, 737–764.
Kaiser, J., Lamy, F., 2010. Links between Patagonian Ice Sheet fluctuations and Antarctic dust variability during the last glacial period (MIS 4-2). Quaternary Science Reviews 29, 1464–1471.
Kaus, B., Castelltort, S., 2013. Numerical Modelling and Analysis of Surface Processes. In: Topomod Short Course Mainz. http://www.topomod.eu/training-courses/topomod-short-course-mainz/.
Kemp, R.A., Toms, P.S., King, M., Kröhling, D.M., 2004. The pedosedimentary evolution and chronology of Tortugas, a Late Quaternary type-site of the northern Pampa, Argentina. Quaternary International 114 (1), 101–112.
Kirby, E., Whipple, K.X., 2012. Expression of active tectonics in erosional landscapes. Journal of Structural Geology 44, 54–75. http://dx.doi.org/10.1016/j.jsg.2012.07.009.
Klein, G.D., 1995. Intracratonic basins. In: Busby, C.J., Ingersoll, R.V. (Eds.), Tectonics of Sedimentary Basins. Blackwell Science, Cambridge Massachusetts, pp. 459–478.
Kröhling, D., 1998. Loess in Argentina: temperate and tropical. In: INQUA International Joint Field Meeting, Excursion Guide No. 2: North Pampa (Carcarañá River Basin, Santa Fe province), Argentina. INQUA-PASH-CLIP-UNER-CECOAL, p. 33. Paraná.
Kröhling, D., 1999. Upper Quaternary Geology of the lower Carcarañá Basin, North Pampa, Argentina. Quaternary International 57–58, 135–148.
Kröhling, D., Iriondo, M., 1999. Upper Quaternary Paleoclimates of the Mar Chiquita area, North Pampa, Argentina. Quaternary International 57/58, 149–163.
Kröhling, D., Iriondo, M., 2003. El loess de la Pampa Norte en el Bloque de San Guillermo. Revista de la Asociación Argentina de Sedimentología 10 (2), 137–150.
Kröhling, D., Brunetto, E., 2013. Capítulo 26. Marco geológico y geomorfología de la cuenca del Arroyo Cululú. In: Bases para el ordenamiento del territorio en el medio rural – Región Centro, Argentina. Parte 3-Territorio Santafesino. Editorial de la Universidad Nacional de Río Cuarto, pp. 485–512.
Kröhling, D., Brunetto, E., Galina, G., Zalazar, M.C., Iriondo, M., 2014. Planation surfaces on the Parana Basaltic Plateau, South America. In: Rabassa, J., Ollier, C. (Eds.), Gondwana Landscapes in Southern South America, Springer Earth System Series. Springer Verlag, pp. 247–304.
Kruck, W., Helms, F., Geyh, M.A., Suriano, J.M., Marengo, H.G., Pereyra, F., 2011. Late pleistocene-holocene history of Chaco-Pampa sediments in Argentina and Paraguay. Quaternary Science Journal 60 (1), 188–202. http://dx.doi.org/10.3285/eg.60.1.13.
Lagarde, J.L., Baize, S., Amorèse, D., Delcaillau, B., Font, M., Volant, P., 2000. Active tectonics, seismicity and geomorphology with special reference to Normandy (France). Journal of Quaternary Science 15, 745–758.
Lagarde, J.-L., Amorèse, D., Font, M., Laville, E., Dugué, O., 2003. The structural evolution of the Channel area. Journal of Quaternary Science 18, 201–213.
Lagorio, S.L., 2008. Early Cretacous alkaline volcanism of the Sierra Chica of Córdoba (Argentina): mineralogy, geochemistry and petrogenesis. Journal of South American Earth Sciences 26, 152–171.
Lague, D., Davy, P., Crave, A., 2000. Estimating uplift rate and erodability from the area–slope relationship: examples from Brittany (France) and numerical modelling. Physics and Chemistry of the Earth 25A, 543–548.
Liu, M., Stein, S., Wang, H., 2011. 2000 years of migrating earthquakes in North China: how earthquakes in midcontinents differ from those at plate boundaries. Lithosphere 3. http://dx.doi.org/10.1130/L129.
Mannavella, C.H., Venencio, M.V., 1995. Influencia de los sedimentos pampeanos en la obra de recarga artificial del acuífero en la ciudad de Sunchales, Provincia de Santa Fe, Argentina, 2do. In: Simposio sobre aguas subterráneas y perforación de pozos en el Paraguay, pp. 137–147. San Lorenzo, Paraguay.
Marotta, G.S., França, G.S., Monico, J.F.G., Fuck, R.A., Araújo Filho, J.O., 2013. Strain rate of the South American lithospheric plate by SIRGAS-CON geodetic observations. Journal of South American Earth Sciences 47, 136–141.
Milani, E.J., Zalán, P.V., 1999. An outline of the geology and petroleum systems of Paleozoic interior basins of South America. Episodes 22 (3), 199–205.
Nash, D.B., 1984. Morphologic dating of fluvial terrace scarps and fault scarps near West Yellowstone, Montana. Geological Society of America Bulletin 95, 1413–1424.
O'Callaghan, J., Mark, D., 1984. The extraction of drainage networks from digital elevation data. Computer Vision Graphics 28, 328–344.
Ouchi, S., 1985. Response of alluvial rivers to slow active tectonic movement. Geological Society of America Bulletin 96, 504–515.
Paola, C., 2000. Quantitative models of sedimentary basin filling. Sedimentology 47 (Suppl. 1), 121–178. http://dx.doi.org/10.1046/j.1365-3091.2000.00006.x.
Pasotti, P., 1974. La Neotectónica en la Llanura Pampeana. Fundamentos para el mapa neotectónico. Instituto de Fisiografía y Geología de la Universidad Nacional de Rosario 58, 1–28.
Pasotti, P., 1975. Nuevo aporte a la Neotectónica de la llanura chaco-pampeana. In: Segundo Congreso Ibero-Americano de Geología Económica 4, Buenos Aires, pp. 301–314.
Pasotti, P., Castellanos, A., 1963. El relieve de la llanura santafesino-cordobesa comprendida entre los paralelos 32° y 32° 30'S desde 62° 45'W hasta el río Paraná. Publicaciones del Instituto de Fisiografía y Geología de la Universidad Nacional de Rosario 47, 1–79.
Peate, D.W., Hawkesworth, C.J., Mantovani, M.S.M., Shukowsky, W., 1990. Mantle plumes and flood-basalt stratigraphy of the Parana, South America. Geology 18, 1223–1226.
Peate, D.W., 1997. The Parana-Etendeka Province. In: Large Igneous Provinces: Continental, Oceanic, and Planetary Flood Volcanism. Geophysical Monograph 100. American Geophysical Union, pp. 217–245.
Pelletier, J.D., 2008. Quantitative Modeling of Earth Surface Processes. Cambridge University Press, Cambridge, p. 304.
Peulvast, J.P., Bétard, F., Lageat, Y., 2009. Long-term landscape evolution and denudation rates in shield and platform areas: a morphostratigraphic approach. Géomorphologie: relief, processus, environnement 2, 95–108.
Quigley, M.C., Cupper, M.L., Sandiford, M., 2006. Quaternary faults of southcentral Australia: palaeoseismicity, slip rates and origin. Australian Journal of Earth Sciences 53, 285–301.
Ramos, V.A., 1999. Plate tectonic setting of the Andean Cordillera. Episodes 22 (3), 183–190.
Ramos, V.A., Cristallini, E.O., Pérez, D.J., 2002. The Pampean flan-slab of the Central Andes. Journal of South American Sciences 15, 59–78.
Rapela, C.W., Pankhurst, R.J., Casquet, C., Fanning, C.M., Baldo, E.G., González-Casado, J.M., Galindo, C., Dahlquist, J., 2007. The Río de la Plata craton and the assembly of SW Gondwana. Earth-Science Reviews 83, 49–82.
Riccomini, C., Peloggia, A.U.G., Saloni, J.C.L., Kohnke, M.W., Figueira, R.M., 1989. Neotectonic activity in the Serra do Mar Rift system (SE Brazil). Journal of South American Earth Sciences 2 (2), 191–192.
Riccomini, C., Assumpção, M., 1999. Quaternary tectonics in Brazil. Episodes 22 (3), 221–225.
Saadi, A., 1993. Neotectônica da Plataforma Brasileira: esboço e interpretação preliminares. Geonomos, Belo Horizonte 1 (1), 1–15.
Saadi, A., Machette, M.N., Haller, K.M., Dart, R.L., Bradley, L.A., de Souza, A.M.P.D., 2002. Map and Database of Quaternary Faults and Lineaments in Brazil. USGS Open-File Report 02-230, p. 59.
Saadi, A., Bezerra, F.H.R., Costa, R.D., Igreja, H.L.S., Franzinelli, E., 2005. Neotectônica na Plataforma Brasileira. In: Souza, C.R.G., Suguio, K., Oliveira, A.M.S., Oliveira, P.E. (Eds.), Quaternário do Brasil. Holos Editora, Ribeirão Preto, pp. 211–234.
Sagripanti, G.L., Schiavo, H.F., Felizzia, J.A., Villalba, D., Aguilera, H.D., Giaccardi, A.D., Membrives, J.A., 2011. Fuertes paleosismos de intraplaca y sus retornos vinculados a la falla Las Lagunas, Sierras Pampeanas de Córdoba. Revista de la Asociación Geológica Argentina 68 (1), 52–70. Buenos Aires.
Schumm, S.A., 1986. Alluvial river response to active tectonics. In: Active Tectonics. National Academy Press, Washington, D.C, pp. 80–94.
Seidl, M.A., Dietrich, W.E., 1992. The problem of channel erosion into bedrock. Catena Supplement 23, 101–124.
Smalley, R., Ellis, M.A., Paul, J., Van Arsdale, R.B., 2005. Space geodetic evidence for rapid strain rates in the New Madrid Seismic Zone of central USA. Nature 435. http://dx.doi.org/10.1038/nature03642.
Sobrero, F.S., Brunetto, E., 2015. Satellite geodetic data in the analysis of the seismic hazard on faults in an intracratonic setting of the SE South America. Miscellanea INGV. Journal of the Istituto Nazionale di Geofisica e Vulcanologia 27, 463–466. Roma.
Talwani, P., 2014. In: Talwani, P. (Ed.), Intraplate Earthquakes. Cambridge University Press, p. 398.
Tucker, G., Lancaster, S., Gasparini, N., Bras, R., 2001. The channel-hillslope integrated landscape development model (CHILD). In: Landscape Erosion and Evolution Modeling. Springer, pp. 349–388.

Please cite this article in press as: Brunetto, E., et al., Analysis of the interaction between neotectonic and surface processes in a low-land intracratonic setting of South America, Quaternary International (2016), http://dx.doi.org/10.1016/j.quaint.2016.06.018

Uliana, M.A., Biddle, K.T., Cedrán, J.C., 1989. Mesozoic extension and Formation de Argentine Sedimentary Basins. AAPG, pp. 599–614.
Wallace, R.E., 1978. Geometry and rates of change of fault generated range fronts, north-central Nevada. Journal of Research of the United States Geological Survey 6, 637–650.
Walling, D.E., Webb, B.W., 1996. Erosion and sediment yield: a global overview. In: Walling, D.E., Webb, B.W. (Eds.), Erosion and Sediment Yield: Global and Regional Perspectives, International Association Hydrology Sciences Publication, 236, pp. 3–20.
Webster, R.E., Chebli, G.A., Fisher, J.F., 2004. General Levalle basin, Argentina: a frontier Lower Cretaceous rift basin. AAPG Bulletin 88 (5), 627–652.
Whipple, K.X., Tucker, G.E., 1999. Dynamics of the stream-power river incision model: implications for height limits of mountain ranges, landscape response timescales, and research needs. Journal of Geophysical Research-Solid Earth 104 (B8), 17661–17674.
Whipple, K., 2004. Bedrock rivers and the geomorphology of active orogens. Annual Review of Earth and Planetary Sciences 32, 151–185.
Whipple, K.X., Meade, B.J., 2004. Controls on the strength of coupling among climate, erosion, and deformation in two-sided, frictional orogenic wedges at steady state. Journal of Geophysical Research 109, F01011. http://dx.doi.org/10.1029/2003JF000019.
Wobus, C., Whipple, K., Kirby, E., Snyder, N., Johnson, J., Spyropolou, K., Crosby, B., Sheehan, D., 2006. Tectonics from topography: procedures, promise and pitfalls. In: Willett, S.D., Hovius, N., Brandon, M.T., Fisher, D.M. (Eds.), Tectonics, Climate and Landscape Evolution: Special Paper. Colorado Geological Society of America, Denver, pp. 55–74.
Yrigoyen, M.R., 1999. Los depósitos cretácicos y terciarios de las cuencas del Salado y del Colorado. In: Caminos, R. (Ed.), Geología Argentina. Instituto de Geología y Recursos Minerales, Buenos Aires, Anales 29(21), pp. 645–649.

Please cite this article in press as: Brunetto, E., et al., Analysis of the interaction between neotectonic and surface processes in a low-land intracratonic setting of South America, Quaternary International (2016), http://dx.doi.org/10.1016/j.quaint.2016.06.018